L.M.Kustov, A.N.Kalenchuk, V.I.Bogdan
Russ. Chem. Rev., 2020, **89** (9) 897 – 916

https://doi.org/10.1070/RCR4940

Systems for accumulation, storage and release of hydrogen

Leonid M. Kustov, Alexander N. Kalenchuk, Viktor I. Bogdan

N.D.Zelinsky Institute of Organic Chemistry, Russian Academy of Sciences, Leninsky prosp. 47, 119991 Moscow, Russian Federation

The results of studies on the hydrogen accumulation, storage and release systems differing in the type of hydrogen interaction with the material (medium) used for hydrogen storage are analyzed. Published data on the use of polycyclic hydrocarbons as the basis for hydrogen storage in a chemically bound state are summarized. Substrate-structure-dependent differences between the mechanisms of heterogeneous catalytic hydrogenation reactions of mono- and polycyclic aromatic hydrocarbons with hydrogen storage capacity > 7 mass % and dehydrogenation of corresponding polycyclic naphthenes are discussed.
The bibliography includes 188 references.

Contents

1. Introduction 897
2. Physical and physicochemical systems for accumulation, storage and release of hydrogen 898
2.1. Compressed hydrogen gas 898
2.2. Liquid hydrogen 899
2.3. Physisorption of hydrogen 899
2.4. Metal hydrides as hydrogen storage materials 900
3. Hydrogen storage in chemically bound state 902
3.1. Systems based on chemical compounds 902
3.2. Systems based on aromatic hydrocarbons 902
3.2.1. The benzene – cyclohexane system 904
3.2.2. The toluene – methylcyclohexane system 906
3.2.3. Systems based on fused compounds 908
3.2.4. Systems based on hydrocarbons with linearly connected rings 911
4. Conclusion 913

1. Introduction

In a relatively short period of time, several 'energy revolutions' associated with the development of new sources and forms of energy (*i.e.* steam engines) have occurred in the history of mankind. Indeed, wood, peat and coal as traditional sources of thermal energy were superseded by various kinds of petroleum and gaseous fuels as main sources of electrical energy; probably, in the future the latter will be replaced by atomic energy.

Energy consumption continuously increases, whereas energy storage and transportation still remain technically challenging. Energy storage in nuclear fuel is hazardous. Modern storage units used for accumulation of mechanical energy (*e.g.*, compressed spring energy, flywheel rotation energy) or electric and magnetic field energy (capacitors, accumulators, coils, *etc.*) are poorly suitable for energy storage applications.[1,2] The potential of utilization of wind energy, tide energy and energy of geothermal sources has natural limitations. A significant part of water resources is already in electricity generation, while solar energy applications in the most economically developed countries are limited by low solar radiation. Alternative fuel sources, including biofuel (bioethanol, biomethanol, biogas, biodiesel) and synthetic fuel (dimethyl ether, methanol, *etc.*), are also limited.[3–5]

Currently, a significant part of energy is produced using petroleum and natural gas. In the context of increased energy consumption, this increases the environmental load. Potential energy sources that can replace or compete with fossil fuel include hydrogen.[6–8] The energy content of hydrogen per unit mass is 120.7 MJ kg^{-1}, being higher than that of any hydrocarbon fuel (*e.g.*, 46 MJ kg^{-1} for petroleum-based fuel). Hydrogen has boundless resources, *viz.*, it ranks second in the number of atoms (~17%) after oxygen (~52%) and ninth (~1%) in mass; the average content of hydrogen in Earth's crust is 1.4 g kg^{-1}.[9] Hydrogen conversion processes are environmentally safe. Hydrogen can be used instead of coal as a reducing agent for iron recovery from ore in steel production, and decarbonization of the process leads to a considerable decrease in harmful emissions of metallurgical production.[10] Mobile applications of hydrogen can be exemplified by the operation of hydrogen fuel cells (HFCs) in automotive and aerospace industry. At present, HFCs are widely used in power engineering. Electrochemical oxidation of hydrogen in HFCs involves a slow stage of dissociative electrochemical adsorption of molecular hydrogen on a platinum electrode

$$H_2 + 2\,Pt \rightarrow 2\,Pt - H_{ads} \quad (1)$$

L.M.Kustov. Doctor of Sciences (Chemistry), Professor, Head of the Laboratory at the ZIOC RAS.
Telephone: +7(499)137 – 2935, e-mail: lmk@ioc.ac.ru
A.N.Kalenchuk. PhD (Physics and Mathematics), Researcher at the ZIOC RAS.
Telephone: +7 (499) 137 – 2935, e-mail: akalenchuk@yandex.ru
V.I.Bogdan. Doctor of Sciences (Chemistry), Leading Researcher at the ZIOC RAS.
Telephone: +7 (499) 135 – 6426, e-mail: vibogdan@gmail.com
Current research interests of the authors: catalysis, nanomaterials, hydrogenation and dehydrogenation processes, green chemistry.

Translation: A.M.Raevskiy

Received 13 January 2020

© 2020 Uspekhi Khimii, ZIOC RAS, Russian Academy of Sciences and IOP Publishing Limited

and a fast electron transfer step

$$2\,Pt-H_{ads} \rightarrow 2\,Pt + 2\,H^+ + 2\,e \quad (2)$$

The reaction is sensitive to CO impurity (~1 ppm) which causes an abrupt increase in the anodic potential and reduces the HFC performance.[11–16]

Pure hydrogen for mobile applications can also be produced and accumulated using electrolysis of water or excess of electrical energy during off-peak hours (at night or on holidays) when the energy consumption decreases.[17] Energy stored in hydrogen can be released at any time by combustion of hydrogen. Progress in hydrogen energetics is, in particular, hindered by the fact that H_2 is a gas of low density (~0.089 g L^{-1}) and high corrosion activity under normal conditions.

Interest in the hydrogen storage problem has grown particularly in the last 15 years. Recent reviews and original publications are devoted to both classical and new concepts of hydrogen storage.[18–27] An analysis of published data revealed no hydrogen storage system that would meet all modern requirements, being fundamentally superior to all other systems. However, from the standpoint of transportation, the storage systems based on hydrogen-containing chemical compounds are considered separately. The density and content of hydrogen in such systems are independent of external factors and therefore hydrogen present in organic compounds can be safely stored and transported over long distances under normal conditions, whereas other systems should meet specific requirements for temperature, pressure, air-tightness and safety.

This review presents an analysis and overveiw of published data on the hydrogen storage systems based on physical, physicochemical and chemical interactions between hydrogen and the storage material (medium). The emphasis is placed on the hydrogen storage and release systems based on heterogeneous catalytic hydrogenation of mono- and polycyclic aromatic hydrocarbons with a storage capacity of more than 6.5 mass % – 7.0 mass % H_2 and on dehydrogenation of corresponding naphthenes. We will discuss the mechanisms of reversible processes depending on the structure of substrates. A distinctive feature of this review is a structured approach to consideration of reactions involving aromatic hydrocarbons and corresponding naphthenes.

The following abbreviations and designations are used in the review:

bcc — body-centred cubic lattice,
CNFs — carbon nanofibres,
CNTs — carbon nanotubes,
D — external diameter of cylinder (tank),
d — cylinder (tank) wall thickness,
E_a — activation energy,
ΔG — Gibbs energy,
ΔH — enthalpy of reaction,
K — equilibrium constant,
NEXAFS — near-edge X-ray absorption fine structure,
ΔP — excess pressure,
PCC — petroleum coke carbon,
R — universal gas constant,
S_{sp} — specific surface area,
ΔS — entropy of a process,
σ — tensile strength of a material.

2. Physical and physicochemical systems for accumulation, storage and release of hydrogen

Storage of large amounts of gaseous hydrogen does not require special conditions and practically does not differ from natural gas storage. Hydrogen can be accumulated in gas holders as well as natural or artificial underground storage tanks.[9] Utilization of H_2 for on-board applications faces certain limitations. For instance, at room temperature and atmospheric pressure, 4 kg of hydrogen necessary for a fuel cell vehicle to cover 200 km occupies a volume of 45 m^3 (this corresponds to a cylinder 5 m in diameter), which goes beyond all reason.[2] Compaction of hydrogen is achieved by cooling below the critical temperature (−239.95 °C) or compression under high pressure. The International Energy Agency targets for an efficient on-board hydrogen storage system are as follows: a storage capacity of at least 5.5 mass % H_2 and a volumetric hydrogen density of at least 40 kg m^{-3} at operating temperatures in the range from −40 to 60 °C and a maximum pressure of 1.2 MPa.[28,29] These values were calculated ignoring the masses of tank, valves, controllers, pipes, pipe hangers, thermal insulation systems, coolers and other auxiliary equipment.

According to the commonly accepted classification, there are physical, physicochemical and chemical methods for hydrogen storage and release. In physical systems, hydrogen does not interact with the storage material. Physicochemical and chemical methods are based on the ability of hydrogen to reversibly interact with the storage material through van der Waals or chemical interactions.

2.1. Compressed hydrogen gas

Storage of compressed hydrogen gas in cylinders offers the following advantages:

— relatively fast refuelling,

— low energy expenditure for hydrogen supply to consumers, and

— no major infrastructure changes required for mobile applications.

However, the effective hydrogen storage capacity is very low. Hydrogen is characterized by very high diffusibility and can penetrate dynamic seals and switching fittings or microcracks. Contact with hydrogen can lead to corrosion embrittlement of metals. Indoors, even a slight leak of hydrogen from cylinders is more hazardous than the leak of petroleum fuel or natural gas.[30] Thickening of cylinder (tank) walls is followed by an increase in its size and mass[31] and, correspondingly, by a decrease in the gravimetric content of hydrogen:

$$\frac{d}{D} = \frac{\Delta P}{2\,\sigma + \Delta P} \quad (3)$$

where d is the wall thickness, D is the external diameter of the cylinder (tank), ΔP is the excess pressure and σ is the tensile strength of the material.

Clearly, at a certain point, a further increase in wall thickness becomes unprofitable; small amounts of compressed hydrogen gas are stored in conventional steel cylinders with operating pressures of up to 15–20 MPa. The energy consumption for compressing gas in a conventional steel cylinder is about 2–3 kW h kg^{-1}, while the

total energy consumption for hydrogen storage exceeds 10%–15% of the calorific power of hydrogen. As a consequence, the content of hydrogen in steel cylinders is at most 1.2 mass %–1.5 mass % and the volumetric hydrogen density is 10–12 kg m^{-3}. Increasing the storage capacity by compressing to high pressures is a complicated engineering problem that remains to be solved. For instance, hydrogen compression at a pressure of 55 MPa causes the hydrogen volume to decrease by 30% (*cf.* 55% at a pressure of 103 MPa); however, the explosion hazard of the method increases substantially.[31] It should be noted that the energy density of hydrogen is much lower than that of petroleum fuel even at so high pressures, *viz.*, 4.7 MJ L^{-1} (1.3 kW h L^{-1}) at a pressure of 70 MPa *vs.* 31.7 MJ L^{-1} (8.8 kW h L^{-1}), respectively.[29] Besides, high-pressure, carbon-fibre hydrogen storage cylinders (tanks) are nearly tenfold more expensive than a petroleum fuel tank of the same volume.

A possible method for storage of compressed hydrogen gas is microencapsulation at pressures in the range of 35–65 MPa. It utilizes low-density glass microspheres 5–500 μm in diameter with nearly 1 μm-thick walls, which can fill any closed space.[32,33] Unlike steel cylinders, in this case the hydrogen volume is redistributed over a large number of small cells; this excludes instantaneous gas blast in case of emergency destruction of the tank. In some cases, the content and volumetric density of hydrogen can be as high as 10 mass % and 20 kg m^{-3}, respectively; however, hydrogen release at the necessary rate is achieved only at temperatures of about 600 °C, at which the glass strength is significantly reduced. To be strong enough, multicapillaries should have a perfect, defect-free surface, which is difficult to prepare and expensive. In addition, there is a problem of switching with gas compressor valves, as well as potential losses during transportation and operation. Taken altogether, this limits the prospects for application of the multicapillary approach as a common method for hydrogen storage.

2.2. Liquid hydrogen

The cryogenic method provides a much higher hydrogen density (70.8 g L^{-1}). Hydrogen as cryogenic liquid exists in a very narrow temperature range from the boiling point (−252.77 °C) to the freezing point (−259.19 °C).[6] The critical pressure for storage of liquid hydrogen is 1.3 MPa and therefore the strength requirements for cryostats are not as stringent as for compressed hydrogen storage tanks; this allows one to achieve high gravimetric content of hydrogen stored (100 mass %).[34,35] The local overheating (hot spot) problem is solved using a portion of cooled hydrogen, which leads to additional energy expenditure and reduces the hydrogen storage capacity. In particular, the storage capacity of aerospace cryogenic systems reaches a value of 85 mass % H_2. The actual storage capacity of small cryostats decreases to 15 mass %–20 mass % H_2 taking account of screen vacuum thermal insulation (a total of 6–8 kg per kilogram of hydrogen with inclusion of the mass of the cryostat). The volumetric density of hydrogen in small cryostats equals that of gaseous hydrogen in carbon-composite cylinders (40 MPa); however, the physical mass of the storage system per kilogram of hydrogen stored is four to five times smaller, which allows such systems to be used for on-board applications.

The drawbacks of the cryogenic method are as follows: high energy consumption for liquefaction of hydrogen (~10 kW h kg^{-1}) and storage of liquid hydrogen and unavoidable evaporation losses (to 5% daily). The total energy cost of hydrogen liquefaction and storage can be as high as 50% of the calorific power of hydrogen.[31] Indoors, evaporation makes the technique more explosion hazardous than storage in steel cylinders. At present, no solution to the hydrogen loss problem is available.

2.3. Physisorption of hydrogen

Physisorption implies that hydrogen is stored within an accumulating matrix through van der Waals forces acting between the sorbent surface and hydrogen molecules. Since the hydrogen–matrix binding energy is low (1–10 kJ mol^{-1}), the storage capacity of adsorbents is at most 1 mass %–3 mass % H_2 under normal conditions and increases only on cooling even for sorbents with a high specific surface area of pores and channels. Elevated pressure favours penetration of hydrogen molecules into micropores. Heating causes the reverse process (desorption) and hydrogen releases from the sorbent without significant difficulties.[36]

The best known adsorbents with a high specific surface area include carbon materials and zeolites, *i.e.*, nonstoichiometric complex aluminosilicates $M_{x/n}(Al_2O_3)_x(SiO_2)_y \cdot m\,H_2O$ (where $2y > x$). The adsorption capacity of zeolites is determined by the structure of the framework, the accessible free-space volume and the nature of the cation representing the binding site of hydrogen molecules. Zeolites can contain a 1D, 2D or 3D system of pores and channels which can occupy up to 50% of the total volume of the material. In spite of this, the storage capacity of zeolites is low (~0.3 mass % H_2) under normal conditions. The adsorption of hydrogen is hampered since pores are blocked by extraframework cations and small pores are inaccessible. At the liquid nitrogen temperature, the storage capacity of different-type zeolites increases to, *e.g.*, 1.8 mass % H_2 for NaY and 2.19 mass % H_2 for CaX. A slight increase in the storage capacity was also observed upon incorporation of metals with high hydrogen binding energies into the zeolite structures.[37–39]

Carbon materials have less ordered structures than zeolites and are by and large characterized by higher hydrogen storage capacity, but only at cryogenic temperatures. For instance, the storage capacity of active carbons that is equal to 7 mass %–8 mass % H_2 in the temperature range from −208.15 to −195.15 °C and a pressure of about 4 MPa decreases to 0.5 mass % H_2 at room temperature.[40–44] Assuming that the hydrogen–matrix binding energy is 10 kJ mol^{-1}, the total energy of the adsorbent and 4 kg of H_2, necessary for a fuel cell vehicle to have a range of 400 km, is ~20 MJ.[6,22] Cooling of this system with liquid nitrogen (−196.15 °C, heat of vapourization is 5.6 kJ mol^{-1}) requires at least ~100 kg of liquid N_2. Such a system is technically difficult to operate; therefore, numerous attempts have been made to design carbon materials with higher hydrogen–matrix binding energies, mainly by increasing the surface area and volume of pores and channels.[45] Carbon nanofibres (CNFs) demonstrated no increase in the CNFs–hydrogen binding energy, probably, due to strong interaction between graphite layers, which precludes the diffusion of hydrogen. As a result, the adsorption storage capacity of CNFs at room temperature remains as low as that of conventional carbon materials (0.7 mass % H_2 at 10 MPa).[46,47] The hydrogen storage capacity increases only upon surface activation; however,

no linear correlation between the storage capacity and the increase in the specific surface area of CNFs was established.

The hydrogen storage capacity of carbon nanotubes (CNTs) does not differ from that of CNFs in spite of the curvature of graphene sheets and the presence of large inner cavities. For instance, the storage capacity of single-walled CNTs with a specific surface area of 2560 $m^2\ g^{-1}$ is less than 1 mass % H_2 under normal conditions and 4 mass % – 5 mass % H_2 at 77 K.[48–50] As for CNFs, no correlation between the specific surface area and the adsorption capacity was found. Depending on the synthesis conditions, the reaction products contain CNTs and other forms of carbon (fullerenes, multi-walled polyhedral nanoparticles, graphite and amorphous carbon nanocrystals — a total of 30% to 80% by mass) that influence the results of experiments.[31]

Great expectations were associated with graphene, a novel carbon material. However, it was shown that graphene has low hydrogen storage capacity (< 1 mass %) similarly to CNTs.[51] The energy barrier to adsorption decreases and, correspondingly, the hydrogen storage capacity increases only upon functionalization of graphene. For instance, a storage capacity of 5.1 mass % H_2 was reported for an Al-doped graphene sheet; however, this is lower than the target values.

A high specific surface area and a large pore volume in metal-organic frameworks (MOFs) are due to the absence of pore walls owing to specific interactions between mono- or polynuclear coordination sites (metal ions) and organic ligands.[52–55] The probability of hydrogen adsorption increases upon formation of additional adsorption sites through the filling of the MOF cavities with organic or inorganic guests. At the same time, the hydrogen storage capacity values of MOFs rarely exceed those of CNTs. For instance, the storage capacity of compound $Zn_4O[O_2C-C_6H_4-CO_2]_3$ (S_{sp} = 3000 $m^2\ g^{-1}$) is 1 mass % H_2 at room temperature and 4 mass % – 5 mass % H_2 at 70 K and a hydrogen pressure of 2 MPa. The MOF-210 and NU-109 samples with a specific surface area of 3200, 6240 and even nearly 7000 $m^2\ g^{-1}$ also demonstrated the hydrogen storage capacities of at most 2 mass %. These and certain other facts were explained in an experimental study[56] where the authors showed that hydrogen adsorption increases with increasing specific surface area only to a value of 2000 $m^2\ g^{-1}$ since larger surface areas cannot be fully covered with hydrogen molecules. Experimental data were confirmed by the results of grand canonical ensemble Monte Carlo calculations.[57,58]

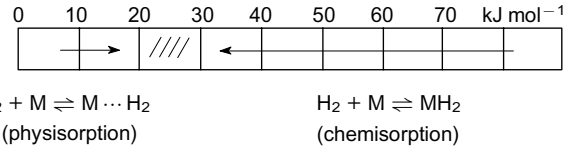
The results obtained demonstrate that a high specific surface area should not be used as the one and only criterion when developing novel adsorbents with high hydrogen storage capacity. Many authors consider the enthalpy of adsorption (ΔH)[59,60] as at least equally important parameter:

$$-RT\ln K = \Delta G = \Delta H - T\Delta S \quad (4)$$

where R is the universal gas constant, T is the temperature of the process, K is the equilibrium constant, ΔG is the Gibbs energy and ΔS is the entropy of the process. At $\Delta G < 0$ and $\Delta H < 0$, the process proceeds spontaneously.

The difference between the enthalpies of hydrogen adsorption (desorption) of the storage systems based on physisorption (1–10 kJ mol^{-1}) and on chemisorption (40–100 kJ mol^{-1}) is illustrated by Scheme 1 which presents the ranges of the hydrogen–storage material interaction energies. A comparison of two outermost values showed that for an optimum storage system based on adsorption materials the energy of the interaction between hydrogen and the storage material should be in the range of 20–30 kJ mol^{-1} under normal conditions.[60] Therefore, investigations of chemical systems should be aimed at synthesizing organic compounds with low energies of hydrogen release.

Scheme 1



M is the storage material

Optimum values of the enthalpies of hydrogen adsorption can be achieved by activating the surface of storage materials through polarization or irradiation.[61,62] In particular, high electric field increases the ability of fullerenes to bind hydrogen, probably, due to the interaction of the charged spherical surface with polarized H_2 molecules.[63,64] Switching off the electric field causes the system to return to the initial state while hydrogen molecules are readily desorbed. It was shown[61] that irradiation favours excitation and activation of the surface and internal adsorption sites, which strengthens the interaction between hydrogen and the surface of the material and improves the sorption properties of the material. The volumes of hydrogen adsorbed on and desorbed from γ-irradiated CNTs increased by about 15% compared to the untreated CNTs.[62]

An analysis of the data obtained in the experiments with adsorption materials demonstrated that, in spite of relatively low cost and simple design, systems for hydrogen accumulation, storage and release based on the physicochemical interaction with porous materials having a high specific surface area still do not meet the technological requirements even if researchers use modern methods of synthesis and surface activation. Such a situation is mainly due to the low density of hydrogen and to the need for cryogenic conditions to increase the hydrogen storage capacity. Few reports on high hydrogen storage capacities of certain new porous nanomaterials characterize particular samples rather than represent the results of systematic studies.[31]

2.4. Metal hydrides as hydrogen storage materials

Metal hydrides contain metal–hydrogen bonds of different energy. The density of hydrogen in certain metal hydrides reaches a value of 170 g L^{-1}, being more than twice as high as the density of liquid hydrogen.[65] Increasing the pressure of gaseous hydrogen and lowering the temperature favours the formation of metal hydrides; otherwise, they decompose.

Considering the types of chemical bonds, there are ionic, covalent and metal hydrides. Typical representatives of the first group include alkali and alkaline-earth metal hydrides (NaH and CaH_2, respectively) with ionic bonds M^+-H^-.[66] The packing density of metal atoms in the structure of ionic hydrides is higher than in the structure of

the parent metals due to contraction of the metal lattice in the course of hydride formation.

Covalent hydrides are usually formed by the low-molecular-mass Group II elements, which predetermines the highest storage capacity among all metal hydrides (*e.g.*, 18.2 mass % H_2 for BeH_2). However, the lack of direct methods for the synthesis by the reaction between hydrogen and the parent metal and irreversible character of decomposition negate the advantage of covalent hydrides as a basis for hydrogen storage systems.

Light-metal alanates $M(AlH_4)_n$ and borohydrides $M(BH_4)_n$, where n is the valence of the metal, are also considered as promising covalent hydrides. However, the storage capacity of these compounds decreases, being, *e.g.*, 7.4 mass % H_2 for sodium alanate $NaAlH_4$ and 10.5 mass % H_2 for lithium alanate $LiAlH_4$. Moreover, as opposed to binary hydrides, hydrogen release from alanates is a multistage process, *e.g.*,

$$6\,NaAlH_4 = 2\,Na_3AlH_6 + 4\,Al + 6\,H_2 \quad (5)$$

$$2\,Na_3AlH_6 = 6\,NaH + 2\,Al + 3\,H_2 \quad (6)$$

As a result, the overall process is characterized by slow kinetics and is reversible under rather severe conditions. In particular, the operating temperatures for $NaAlH_4$ decomposition are as follows: from 185 to 230 °C for the first stage and to nearly 260 °C for the second stage; NaH decomposes only at 425 °C. As to $LiAlH_4$, about 2.65 mass % of the total content of hydrogen is retained in LiH after two stages of decomposition (LiH completely decomposes at temperatures above 680 °C). Like the synthesis of a simple aluminium hydride AlH_3, that of $LiAlH_4$ requires elevated pressures.[65] Therefore, in spite of the high initial storage capacity, alanates are not promising materials for hydrogen storage applications.

Aluminium borohydride $Al(BH_4)_3$ is characterized by the maximum volumetric hydrogen density (150 kg m^{-3}) while $LiBH_4$ is characterized by the maximum gravimetric hydrogen density (18.4 mass %) under normal conditions.[67–69] However, as in the case of alanates, intense hydrogen desorption from these borohydrides begins at temperatures above 400 °C. The amount of hydrogen desorbed from $LiBH_4$ at moderate temperatures (100–200 °C) corresponds to a storage capacity of merely 0.3 mass % H_2. Complete release of hydrogen occurs only at about 500 °C, while the total amount of H_2 desorbed at temperatures below 600 °C in the hydrogenation–dehydrogenation cycle is at most half its content in the parent material (9 mass % H_2). In addition, dehydrogenation is accompanied by the formation of stable intermediate products (including toxic diborane B_2H_6). The reverse reduction process requires high energy consumption and thus becomes much less efficient. In some cases the yield of $M(B_{12}H_{12})_{n/2}$-type intermediates is decreased by stabilizing $M(BH_4)_n$ giving polycationic borohydrides $MM'(BH_4)_n$, where M and M′ have different electronegativities.[70–72] It is assumed that in the future combining cations in such a manner can become an efficient method for controlling the thermodynamic stability of metal borohydrides similarly to conventional doping of hydrogen-accumulating alloys. Besides, borohydrides in the nano state can be prepared and preserved by incorporating into nanoporous substrates. In particular, researchers succeeded in reducing the temperature of hydrogen desorption from NH_3BH_3 (16 mass % H_2) and the amount of borazine formed; however, the kinetics of the process is very low.[73] It was also found[74] that the addition of water causes a tenfold increase in the hydrogen release rate; the effect is most probably due to destabilization of the $BH^{\delta-}\cdots{}^{\delta+}HN$ bonds in the crystal lattice of NH_3BH_3 by polar H_2O molecules. The reaction affords polyaminoborane as a side product.

Among metal hydrides, MgH_2 (7.6 mass % H_2) is best known. Like other simple metal hydrides MH_x, hydrogen in MgH_2 donates its electron to the metal, which in fact leads to formation of a metal-hydrogen alloy; dehydrogenation of the alloy is characterized by high enthalpy ($\sim$90 kJ mol^{-1} with respect to H_2) and proceeds at high temperatures and pressures (250–350 °C, 5–10 MPa). Also, high density of magnesium hydride makes its surface hardly permeable to hydrogen; as a consequence, the kinetics of hydrogen uptake and release slows down.[75] The available methods for eliminating these difficulties do not solve the problems of reducing the mass of the system and the need to provide special conditions for hydrogen transportation in the form of MgH_2.

Yet another well-known simple metal hydride is AlH_3, which is characterized by low enthalpy of desorption of H_2 (5–8 kJ mol^{-1}). However, a direct synthesis of this compound from aluminium and hydrogen requires very high pressures.

Considerable interest in the low-temperature AB_5 ($CaCu_5$ structural type), AB_2 (Laves phases) and AB (CsCl structural type) metal hydrides as well as pseudobinary hydrides of certain vanadium-based alloys (VH_2) and the Ti–Cr system with the body-centred cubic (bcc) lattice is due to favourable thermodynamics in the relatively comfort range of hydrogen absorption energies (30–43 kJ mol^{-1}) and to high hydrogen adsorption/desorption rates at moderate pressures and temperatures.[76] In the AB_5 compounds, the A component is a rare-earth metal (*e.g.*, $LaNi_5H_x$) and(or) calcium, while in the AB_2 and AB compounds these are titanium subgroup elements; the B component is usually a transition metal (Fe, Ni, Co, V, Mn, Cr, *etc.*), most often, nickel as a good catalyst for the dissociation of H_2.[31] For these hydrides, the equilibrium pressure of hydrogen above the atmospheric pressure is attained at temperatures below 100°C; therefore, the adsorption–desorption processes are characterized by low energy cost. However, high atomic masses of metals cause the gravimetric density of hydrogen to appreciably decrease relative to the total mass and size of the storage systems based on these hydrides. For instance, the storage capacity of $LaNi_5H_x$ ($x = 6–7$) is at most 1.4 mass % H_2 at a volumetric density of 85 kg m^{-3} while that of bcc alloys in the Ti–Cr system is 2.5 mass %–3 mass % H_2.

A comparison of different hydrides as hydrogen storage materials showed that the main advantage of hydride-based storage systems consists in compact equipment since the volumetric density of hydrogen in the metal matrix (90–100 kg m^{-3}) is higher than in liquid hydrogen and comparable with the density of hydrogen in water (110 kg m^{-3}). Also, the metal hydride approach is safe because the pressure of gaseous hydrogen over the vast majority of metal hydrides at room temperature is at most a few atmospheres. However, high atomic masses of metals predetermine a large size of the metal hydride-based hydrogen storage systems; this considerably reduces the hydrogen storage capacity. An additional problem consists in the brittle behaviour of the metals interacting with hydrogen.

3. Hydrogen storage in chemically bound state

3.1. Systems based on chemical compounds

Unlike the storage systems based on physical and physicochemical interactions of hydrogen with the storage material, in chemical systems hydrogen is a constituent of organic compounds and therefore its content and density are independent of external factors, being determined by the nature and structure of a particular compound. Hydrogen present in chemical substrates can be safely stored and transported over long distances under normal conditions as well as released and converted to other forms of energy when necessary. Typical examples of chemical substrates with high volumetric hydrogen density (>100 kg m^{-3}) and gravimetric hydrogen density are provided by ammonia (17.6 mass % H_2) and methanol (12.6 mass % H_2) that are produced on a large scale.

Remind that the synthesis of ammonia and production of hydrogen from ammonia are energy-consuming processes. The former is an exothermic reaction which proceeds at high pressures and temperatures, the yield of ammonia being usually at most 14%–16% per reaction cycle. The Haber–Bosch process[77] enables a nearly 100% conversion of atmospheric nitrogen to ammonia; however, the average electrical energy consumption exceeds a value of 3200 kW h.

Catalytic decomposition of ammonia into molecular nitrogen and hydrogen

$$2\,NH_3 = N_2 + 3\,H_2 - 92\ kJ \qquad (7)$$

occurs at 900 °C. This is an endothermic reaction that can be maintained using a portion of the released hydrogen. In this case the efficiency of the system for hydrogen production and storage is 60%–70% of the efficiency of the system that operates using no released hydrogen. On the other hand, compression of ammonia requires 20–25 times higher installed capacity compared to compression of hydrogen (at a compressor efficiency of 75% for both gases). An undoubtful advantage of ammonia[78] manifests itself only in comparison with the storage and transportation of liquid hydrogen since the number of hydrogen atoms in one litre of liquid anhydrous ammonia is larger than in one litre of liquid hydrogen. The liquefaction temperature of ammonia is only −33.39 °C (critical temperature is 131.85 °C) and it can be liquefied with ease at ambient temperature and a pressure of 1.0 MPa. However, taking into account high energy expenditure for the synthesis and decomposition, ammonia, as a storage system, loses its advantages over aromatic hydrocarbons with high hydrogen storage capacity.

The efficiency of hydrogen production from methanol and subsequent storage is also 65%–70%;[79] however, the released hydrogen contains CO_x impurities

$$MeOH = CO + 2\,H_2 \qquad (8)$$

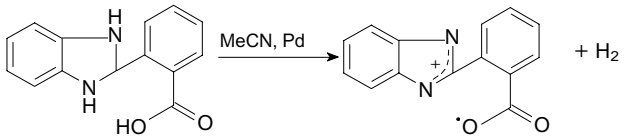
$$H_2O + CO = CO_2 + H_2 \qquad (9)$$

Catalytic decomposition of MeOH and conversion of CO are endothermic processes proceeding at 400–600 °C and atmospheric pressure. Steam conversion of methanol proceeds under milder reaction conditions, namely, at 70–350 °C. These temperatures are lower than the temperature of steam conversion of methane; therefore, the energy consumption for production of hydrogen from methanol is about 20% lower compared to natural gas. However, in both cases the cost of hydrogen purification from associated gases is high.

Among new chemical systems for hydrogen storage and release, there are formic acid and ionic liquids. Interest in the use of the former compound followed the development of a one-step method for its synthesis from hydrogen and atmospheric carbon dioxide.[80,81] Traditionally, formic acid is obtained in a multistage process accompanied by the formation of undesired side products. However, formic acid has a low flash point (60 °C) and low hydrogen storage capacity (4.3 mass %). Formic acid, ammonia and methanol are also of limited use for hydrogen storage systems because of their aggressive behaviour and toxicity; indeed, one of the main reasons for the interest in hydrogen is environmental safety. In addition, in this case hydrogen should be purified from associated gases.

Unlike formic acid, imidazolium ionic liquids containing cyclohexane moieties {*e.g.*, 1-methyl-3-[3-(cyclohexyl)propyl]imidazolium bis(trifluoromethylsulfonyl)imide} are nonflammable in operation because of low vapour pressure, high density, chemical and thermal stability.[82,83] Dehydrogenation of benzimidazolines (*N*,*N*′-dimethyldihydrobenzimidazole, 1,3-dimethyl-2-phenylbenzimidazoline or 1,3-dimethylbenzimidazoline) on Pd catalysts in acetonitrile produces small amounts of hydrogen already at room temperature. As an example, Scheme 2 presents the reaction scheme for hydrogen release from 2-(2-carboxyphenyl)benzimidazoline.

Scheme 2

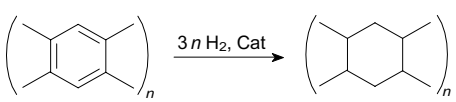


Using imidazolium ionic liquids, a volumetric hydrogen density to 30 g L^{-1} at atmospheric pressure was attained;[6] this value is nearly twice as high as the volumetric density of hydrogen compressed at a pressure of 35 MPa. However, dehydrogenation of compounds in question proceeds in fact irreversibly and the complete release of hydrogen takes an unacceptably long time of at least 100 h.

3.2. Systems based on aromatic hydrocarbons

Among chemically bound hydrogen storage systems, 'organic substrate–catalyst' composites based on aromatic hydrocarbons with a storage capacity higher than 7.2 mass % H_2, capable of participating in catalytic hydrogenation–dehydrogenation reactions (Scheme 3), are of principal interest.[6–8]

Scheme 3



The foundations of hydrogenation catalysis of organic compounds were developed in the late 19th–early 20th century by Sabatier and Zelinsky.[84] More recently, Ipatieff[85] established that the hydrogenation reaction rate

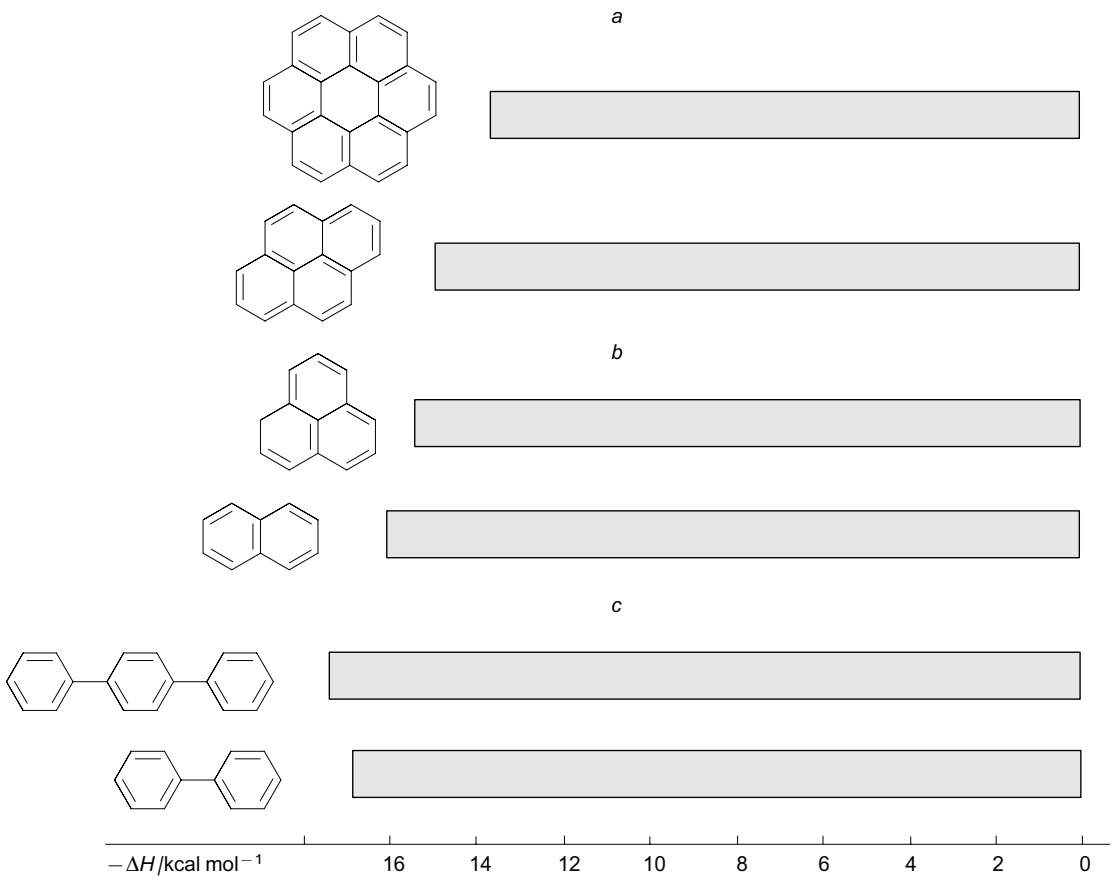


Figure 1. Enthalpies of hydrogenation of differently fused aromatic compounds plotted *vs.* the number of unsaturated hydrocarbon rings.[95] For *a*–*c*, see text.

depends on the hydrogen pressure. At present, catalytic hydrogenation processes based on Ipatieff's principles belong to the key processes in chemical industry. Meanwhile, actualization of environmental problems contributes to a fundamentally new application of classical hydrogenation–dehydrogenation reactions, which differs from traditional views on the use of hydrogenation processes.[86–88] The hydrogen storage systems based on aromatic hydrocarbons allow one to avoid most limitations on pressure, temperature, volatility and safety inherent in physical and physicochemical methods.[89,90]

Dehydrogenation of naphthenes is energetically more favourable than dehydrogenation of linear aliphatic molecules since arenes formed in the reaction are characterized by increased stability of the aromatic system.[91] The necessary purity of hydrogen is ensured by selective catalysts based on Group VI and VIII transition metals (or by these metals *per se*) that allow one to carry out reactions without formation of side products and CO_x gases.[92–94] Studies on aromatic hydrocarbons as a basis for reversible hydrogen storage systems have been started quite recently.

Currently, substrates for hydrogen storage systems based on catalytic hydrogenation–dehydrogenation reactions are mainly chosen using the energy approach. According to this approach, a decrease in the dehydrogenation temperature (this is of importance for operation of fuel cells) is possible for those naphthenes whose π-conjugated aromatic analogues meet the following condition: the absolute value of changes in the enthalpy of hydrogenation $|\Delta H|$ is less than 15.0 kcal mol^{-1} (62.8 kJ mol^{-1}) with respect to H_2.[95] Taking simple polycyclic (Fig. 1 *a*), fused (Fig. 1 *b*) and linearly connected (Fig. 1 *c*) aromatic compounds as examples, one can see that this criterion is best met by the polycyclic and fused compounds.[8] Moreover, according to quantum chemical calculations,[95] the $|\Delta H|$ values for these types of compounds decrease with increasing number of unsaturated hydrocarbon rings.

Considering a 100% conversion of simple naphthene substrates into π-conjugated aromatic hydrocarbons (*e.g.*, dehydrogenation of (i) cyclohexane to benzene or (ii) decalin to naphthalene), the total amount of the released hydrogen is ~7.2 mass % (*cf.* 7.4 mass % for perhydroanthracene or coronene). However, these compounds are poorly hydrogenated and dehydrogenated. In particular, the amount of hydrogen released in the dehydrogenation of pentacene ($C_{22}H_{14}$) † and coronene ($C_{24}H_{12}$) under identical conditions corresponds to a storage capacity of 0.15 and 1 mass % H_2, respectively.[95] Hydrogenation of fullerene C_{60} affords, *e.g.*, compound $C_{60}H_{48}$ with a maximum hydrogen content of 4.5 mass %–6.3 mass %, which is lower than the storage capacity of conventional polycyclic hydrocarbons. To date, all attempts to synthesize and characterize hydrofullerene $C_{60}H_{60}$ with a storage capacity of 7.7 mass % H_2 failed;

† We believe that the molecular formulas of the compounds in question facilitate a visual comparison of these systems based on the C/H atom ratio.

probably, this is due to instability of the compound owing to excess steric strain.[96]

In this connection it is appropriate to mention that, from the standpoint of accumulation, storage, transportation and release of hydrogen, the requirement for cyclic character of hydrogenation and dehydrogenation of polycyclic hydrocarbons without loss of substrates differentiates these reactions from traditional hydrogenation catalysis. Solution to the problem thus formulated depends on the development of the 'substrate–catalyst' composite system whose components are suitable for 100% saturation in the hydrogenation step and subsequent release of hydrogen without formation of side products. The latter pollute the released hydrogen, which can lead to decomposition and loss of the substrate; this reduces the operating life of the hydrogen storage system.

A catalytic reaction involves a number of successive stages including adsorption, desorption, diffusion, dissociation and reaction *per se*; therefore, knowledge of specific features of each stage is of great importance for optimizing the process. Usually, a heterogeneous catalyst has a nonuniform surface with various types of active sites. Since complex organic molecules (*e.g.*, aromatic or naphthene hydrocarbons) can be differently oriented relative to the catalyst surface, only molecules with a particular spatial configuration can enter reactions on certain types of active sites.[97–100] Ordered structures were experimentally detected in a number of systems. For instance, an ultrahigh vacuum scanning tunnelling microscopy study of adsorption monolayers of *p*-hexaphenylene molecules on the Au(111) surface showed that the molecules can be either arranged parallel to the surface or be differently tilted to it.[97] It follows that efficient chemical systems for storage and release of hydrogen should be developed taking account of the structural factor.

In modern theoretical organic chemistry the properties of molecules are interpreted in terms of displacement of valence electrons with inclusion of five effects, *viz.*, the electric field effect as well as the σ-inductive, π-inductive, mesomeric and electromeric effects. Hammett[101] showed that correct results can be obtained taking account of two of them provided that correlations between the structure and physicochemical properties of molecules are known.

The idea of the mechanism of a catalytic process can be obtained using structurally similar compounds characterized by successive changes in the molecular size and shape. Since the stability of all aromatic compounds is governed by the state of the constituent benzene rings, a comparison of the hydrogen storage systems based on polycyclic hydrocarbons is impossible without studying the simplest analogues to polycyclic systems, namely, two pairs of monocyclic compounds, benzene–cyclohexane and toluene–methylcyclohexane. Catalysts for which reaction mechanisms were confirmed experimentally are of great importance.

3.2.1. The benzene–cyclohexane system

The gravimetric density of hydrogen in the benzene–cyclohexane system (two monocyclic compounds) is 7.14 mass %. Both substrates are liquids under normal conditions; however, high saturated vapour pressure (12.7 kPa for benzene and 13.0 kPa for cyclohexane) favours removal of hydrogen stored in cyclohexane.[102] This makes the hydrogen storage system less safe.

According to X-ray and spectral analysis data, benzene (C_6H_6) is a planar molecule. Six carbon atoms form a regular hexagon with equivalent σ-bonds. All of the carbon–carbon bonds are formed as a result of the overlap of $C(sp^2)$ atomic orbitals. Delocalization of electrons in the benzene molecule over six centres makes them completely indistinguishable and gives the most stable electron density distribution in the closed π-system. The stabilization energy of the benzene molecule is 150.7 kJ mol^{-1};[103] all C–C bonds in this molecule are 1.397 Å (0.139 nm), being shorter than the arithmetic mean of the single (1.544 Å) and double (1.337 Å) bond lengths.[103–105]

In the molecule of cyclohexane (C_6H_{12}) the C–C–C bond angle equals 111.08°, being larger than the tetrahedral angle (109°28′), while the C–C bonds 1.528 Å long are shorter than the single bonds.[103–105] At room temperature, more than 99% of cyclohexane molecules in the equilibrium mixture of conformers adopt a chair conformation that is 20–25 kJ mol^{-1} more stable than the boat conformation. In the former conformation, equatorial and axial hydrogen atoms alternate, so there are three 'up' and three 'down' hydrogens. Equatorial atoms are directed radially from the ring towards the molecular periphery, while axial atoms deviate from the ring plane by about 1°. The torsion angles are equal to 55.9°, while the C–H bonds are 1.119 Å.

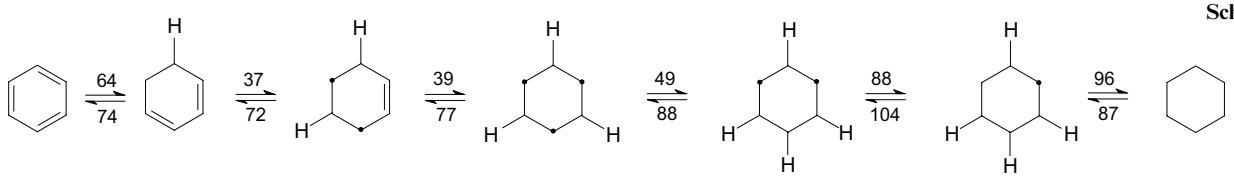
Actual dimensions of the benzene and cyclohexane molecules are such that several reacting atoms approaching the catalyst surface cannot simultaneously contact with one active metal atom. Therefore, the interaction between the reacting molecule and the active metal atom only leads to adsorption since the molecule is insufficiently activated to participate in the reaction. Among the best catalysts for reversible hydrogenation–dehydrogenation of benzene and cyclohexane, there are homogeneous iridium catalysts $IrH_2[C_6H_3\text{-}2,6\text{-}(CH_2PBu^t_2)_2]$.[89] However, high cost, rapid deactivation and losses upon removal of reaction products make these catalysts of limited use for hydrogen storage applications.

In accordance with Balandin's multiplet theory of catalysis, hydrogenation of benzene on the surface of a heterogeneous catalyst proceeds in either in-plane or edgewise fashion (sextet and doublet models, respectively).[106] In the case of in-plane chemisorption, the six-membered ring of the benzene molecule can be flatly superimposed on the metal surface only if the crystal structure of the metal has a face where atoms occupy vertices of equilateral triangles (multiplets) and the interatomic distances fall in certain intervals. If the interatomic distances go beyond these intervals, hydrogen atoms in the benzene molecule become too distant from the metal atoms, which precludes adsorption, and the six-membered ring cannot be perfectly superimposed on the crystal face. Correspondence between the metal lattice constant (a) and geometric parameters of cyclohexane (benzene) molecules is possible for a small group of metals with cubic (A1) and hexagonal (A3) lattices:

Metal	Pt	Pd	Ir	Rh	Cu	Co	Ni
a/Å	2.78	2.75	2.71	2.69	2.56	2.51	2.49

Nearly identical atomic arrangement in these metal lattices and on small surface areas containing a few atoms can be explained by a trend towards the closest packing. In the case of cyclohexane dehydrogenation, flat superimposition is due to the fact that the chemisorption forces acting during the formation of the active complex of cyclohexane

Scheme 4



with the catalyst are stronger than the forces that tend to retain the initial conformation.

The maximum hydrogen release rate (3800 mmol H_2 per gram of metal per minute) for cyclohexane dehydrogenation was obtained in a flow reactor on the Pt/Al catalyst (3 g of Pt per m^3 of catalyst; Al is anodized aluminium) at 375 °C.[107] A decrease in temperature to 300°C caused the hydrogen release rate to decrease to 1900 mmol H_2 per gram of metal per minute.[108] A comparable hydrogen release rate (1800 mmol H_2 per gram of metal per minute) was achieved on the heterogeneous catalyst 3.8% Pt/AC (AC is activated carbon) at 300 °C.[107] An increase in the platinum concentration to 10 mass % led to a decrease in the hydrogen release rate to 510 mmol H_2 per gram of metal per minute. The use of the bimetallic catalysts Pt–Mo/PCC, Pt–W/PCC and Pt–Re/PCC instead of the Pt/PCC system (PCC is petroleum coke carbon) increased the conversion of cyclohexane. Replacement of platinum by nickel led to an abrupt decrease in the hydrogen release rate (7.1, 8.1 and 6.8 mmol H_2 per gram of metal per minute for the Ni/C catalysts containing 10 mass %, 20 mass % and 40 mass % Ni, respectively). As 0.5 mass % Pt was added to the 20% Ni/C catalyst, the cyclohexane conversion increased and the content of cracking products noticeably decreased.[108] Presumably, improvement of the dehydrogenation kinetics upon adding the second metal to the catalyst is due to promotion of C–H bond cleavage and(or) desorption of aromatic products.[109]

Bimetallic catalysts were proposed by inventors from the USA[110] who succeeded in improving the activity of a Re–Pt catalyst in the reforming reaction compared to that of the Pt catalyst by adding a small amount of rhenium to platinum. Physical mixing of the Pd/PCC and Pt/PCC catalysts also increased their activity.[99] Such a mixture utilized the ability of palladium to suppress the reverse reaction and the high hydrogen recombination activity of platinum to achieve a synergistic effect of spillover and hydrogen migration and recombination over Pt and Pd. However, in spite of the synergistic effects observed, the activity improvement mechanism of the catalysts in question was not described, in particular, due to the complex structure of the catalysts (catalyst surface demonstrates differently arranged faces and defects). To simplify the solution to the problem, the Pt(111) single-crystal surface is often used as a model for a real catalyst.[111]

It was hypothesized that hydrogenation of benzene involves successive addition of hydrogen atoms to the benzene molecule adsorbed on the catalyst to give cyclohexadiene, cyclohexene and cyclohexane.[112] The free energies of these reactions at 550 K are 82.1, −42.7 and −39.4 kJ mol^{-1}, respectively,[113] benzene conversion into cyclohexadiene being the rate-limiting step. An alternative approach treats the hydrogenation of benzene as the interaction of adsorbed hydrogen with an aromatic compound.[114]

All elementary events of the benzene hydrogenation reaction were analyzed[115] and the activation energy of each elementary enent of benzene hydrogenation and cyclohexane dehydrogenation was evaluated using quantum chemical calculations in terms of the density functional theory (Scheme 4; the numbers at arrows denote the activation energy values in kJ mol^{-1}).

The Pt(111) single-crystal surface was chosen as a model catalyst, which significantly simplified calculations compared to the calculations of the process on a heterogeneous catalyst. It was shown that the successive conversion of benzene into hydro-, dihydro-, trihydro-, tetrahydrobenzenes, cyclohexyl and cyclohexane is characterized by the lowest energy expenditure. The activation energies for the addition of the first (E_a = 64 kJ mol^{-1}) and (especially) the last hydrogen atom (E_a = 96 kJ mol^{-1}) are higher than the activation energies of the intermediate stages. The addition of the last hydrogen atom is the rate-limiting stage of benzene hydrogenation. For cyclohexane dehydrogenation, the activation energy for each stage is by and large higher than for benzene hydrogenation. The maximum value E_a = 104 kJ mol^{-1} was found for cyclohexyl conversion into tetrahydrobenzene, which is consistent with Balandin's multiplet theory of catalysis.

In accordance with the sextet model, the absence of cyclohexadiene and cyclohexene in gas phase samples is due to the fact that flatly adsorbed cyclohexane molecules are converted into benzene ones upon abstraction of all the six hydrogen atoms in such a manner that the six-membered ring resides at the active site until complete transformation to the benzene ring. Having one hydrogen atom abstracted from the carbon atom, the second H atom executes stretching vibrations along the line of the C–H bond parallel to the surface. If the vibrational amplitude exceeds a certain limit, the second hydrogen atom is abstracted and subsequently combines with the first hydrogen atom. The abstraction of the second hydrogen atom determines the energy barrier to the overall dehydrogenation reaction. Interestingly, the rate-limiting stages of the hydrogenation and dehydrogenation reactions are different.

A complete conversion of cyclohexadiene requires a particular orientation of the molecule being adsorbed on the Pt(111) surface.[116] The chemisorbed carbonized layer of reaction products on the platinum surface acts as a promoter and facilitates the desorption of reaction products; however, it inhibits the process under particular conditions. The H–H and C–H bonds dissociate on one type of active sites, while C–C bonds are cleaved on some other active sites on the platinum surface. At the same time, oxidative treatment of the catalyst favours changes in the electronic structure of the surface of the Pt catalyst, while certain additives (*e.g.*, oxygen) favour acceleration of and selectivity enhancement for both direct and reverse reactions. At high pressures, the presence of terraces and cleavage fractures on the catalyst surface enhances the stability of the surface against the formation of a chemisorbed carbonized layer compared to the single-crystal surface. The apparent activation energies of the reaction at high and low pressures are different because of different reaction mechanisms. In

particular, the chemisorption of cyclohexane requires a group of at least five platinum atoms, whereas the dehydrogenation of adsorbed cyclohexane requires at least eight free platinum atoms.[117]

3.2.2. The toluene–methylcyclohexane system

A good example of changes in the behaviour of substituted hydrocarbons compared to benzene is provided by the toluene ($C_6H_5CH_3$)–methylcyclohexane system[118] that can be treated as a simplified model for more complex polycyclic objects. It should be noted that both compounds are liquid substrates under normal conditions but the system initially has a lower hydrogen storage capacity (6.12 mass %) due to the presence of a methyl group. The saturated vapour pressure of toluene and methylcyclohexane (3.8 and 6.2 kPa, respectively)[102] is lower than that of benzene. Taking account of this fact, many researchers use just this pair of substrates as a basis for a hydrogen storage system.

In benzene homologues, donor substituents havung a positive inductive effect (including methyl groups) cause deformation of σ-bonds in the hydrocarbon ring and an increase in the degree of delocalization of positive charge of the σ-complex compared to the unsubstituted π-complex of benzene.[118] Redistribution of the electron density leads to an increase in the stabilization energy of a toluene molecule to ~163 kJ mol^{-1} (Ref. 103) compared to that of benzene and to acceleration of hydrogen substitution at *meta*- and *para*-positions. The bulky substituent impedes the reaction at *ortho*-position due to van der Waals repulsion.

Hydrogenation of toluene on Pt and Pd catalysts was modelled by analogy with that of benzene as successive addition of dissociatively adsorbed hydrogen to an associatively adsorbed aromatic compound.[119] Toluene loses aromaticity upon the addition of the first hydrogen atom, this stage being the rate-determining for the formation of a non-aromatic intermediate. This mechanism implies a non-competitive adsorption of hydrogen and the aromatic compound. An alternative mechanism involves the formation of a complex of the adsorbed aromatic compound with active sites on the catalyst surface and hydrogen.[120] This scheme was successfully used in the studies of hydrogenation of ethylbenzene and *m*-xylene.

In accordance with Balandin's multiplet theory of catalysis, one-step dehydrogenation of mono- and polysubstituted cyclohexane homologues with simultaneous abstraction of all hydrogen atoms requires that all substituents be on the same side relative to the ring plane.[94] For methylcyclohexane, this condition is met since this molecule exists in the chair conformation and up to 95% of methyl substituents are equatorial in the equilibrium state.[103]

Pioneering investigations of toluene hydrogenation and methylcyclohexane dehydrogenation were carried out by Zelinsky.[84] In the 1960s, Sinfelt contributed largely to studies on the mechanism of methylcyclohexane dehydrogenation.[121] It was established that the reaction is characterized by high selectivity, being zero-order with respect to hydrogen and nearly zero-order with respect to methylcyclohexane. The activation energy for toluene desorption (138.1 kJ mol^{-1}) was found to be different from the heat of adsorption of methylcyclohexane (125.5 kJ mol^{-1}). The authors failed to explain this difference based on 100% surface coverage and therefore proposed a two-step reaction mechanism instead of the one-step mechanism with simultaneous abstraction of all hydrogen atoms (according to Balandin). The new mechanism involves adsorption of toluene produced from methylcyclohexane on the catalyst surface followed by its desorption to the gas phase. The activation energy of the dehydrogenation reaction was calculated as the difference between the two values listed above: 138.1 – 125.5 = 12.6 kJ mol^{-1}.

The kinetics of methylcyclohexane dehydrogenation on the Pt, Pt–Re and Pt–Pd catalysts supported on γ-Al_2O_3 can be described[122] using the Horiuti–Polanyi model[123] that was developed to describe the kinetics of ethylene hydrogenation on Ni catalysts. Three kinetic models were proposed,[124] one based on the Horiuti–Polanyi model and two models with allowance for the surface reactions on the Pt/Al_2O_3 and $Pt–Re/Al_2O_3$ catalysts with one and two active sites, respectively. It was established that conversion of adsorbed methylcyclohexadiene into adsorbed toluene is the rate-limiting stage of the reaction on the Pt/Al_2O_3 catalyst, while the reaction on the $Pt–Re/Al_2O_3$ catalyst produces methylcyclohexene from adsorbed methylcyclohexane.

A study[125] of 11 possible pathways of methylcyclohexane dehydrogenation allowed the authors to propose the optimized reaction mechanism involving the following main stages:

— adsorption of methylcyclohexane on the catalyst surface;

— dehydrogenation of adsorbed methylcyclohexane involving several steps of adsorption; and

— desorption of toluene.

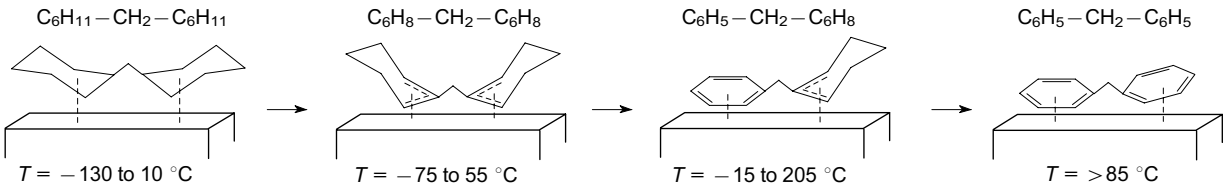
The activation energy for the reaction on the Pt–Re/γ-Al_2O_3 catalyst was 51.9 kJ mol^{-1}. It was assumed that the reaction rate is not influenced by external and internal diffusion, but the effect of diffusion could not be ruled out owing to large particle sizes; probably, this was the reason for the low effective activation energy.

The authors of a mathematical model with inclusion of inter- and intraphase temperature gradients in a fixed bed reactor reported[126] that the dehydrogenation reaction on the (0.25 mass % Pt–0.25 mass % Re)/Al_2O_3 catalyst is of negative order with respect to methylcyclohexane. This was associated with deactivation of the catalyst. To improve the stability of the catalyst against deactivation, the catalyst preparation step was performed under pH control of chloroplatinic acid to achieve uniform platinum distribution within the pores of the support in the course of impregnation. It was shown that controlled high dispersity of platinum favours retention of the activity of the single-component catalysts 0.1 mass %–0.6 mass % Pt/γ-Al_2O_3 even at low content of the active component. Dehydrogenation of methylcyclohexane on the 0.1 mass % Pt/Al_2O_3 catalyst at 350°C was characterized by a high hydrogen release rate (958 mmol H_2 per gram of metal per minute) at a substrate conversion of 99% and a toluene selectivity of 99%. These high values are probably due to hydrogen spillover.[127]

A study[128] on the effect of hydrogen addition on the dehydrogenation of methylcyclohexane revealed the formation of a carbonized layer in the absence of hydrogen and a lower rate of this process upon adding hydrogen.

Sterba and Haensel[129] reported a positive effect of poisoning of the catalyst with sulfur on the activity of the catalyst. However, the effect is not always manifested, *e.g.*, sulfiding of Pt/Al_2O_3 did not lead to an increase in the methylcyclohexane dehydrogenation rate.[130] Toluene formed in the reaction behaved as an inhibitor, the inhib-

Scheme 5



itory ability being increased with temperature and decreased with the pressure of hydrogen.

The authors of a study [131] on methylcyclohexane dehydrogenation on Mo catalysts established that dissociation of hydrogen during the reduction of MoO_2 favours the formation of Brønsted acidic sites Mo–OH and a shift of the thermodynamic equilibrium towards dehydrogenation of methylcyclohexane. The reaction on partially reduced molybdenum oxide (noble-metal-free catalyst) carried out in the temperature range of 300–380 °C gave low conversions. An investigation of the efficiency of bimetallic Pt/Mo catalysts at different Pt/Mo ratios demonstrated [132] an increased activity of the Pt/Mo–SiO_2 catalyst containing 5 mass % Pt and 8 mass % Mo. This was associated with high dispersity of the MoO_2 and Pt^0 phases. Reduction of the catalytic activity at a higher Mo content (10.6 mass % and 12.7 mass %) was explained by the formation of MoO_x–Pt core/shell nanoparticles, which was detected using physicochemical methods.

These data show that even in the case of a relatively simple system, such as toluene–methylcyclohexane, one deals with a large scatter of calculated apparent activation energy values and different interpretations of the reaction mechanism. It should be noted that the strict verification of the mechanisms of reactions of cyclic hydrocarbons on the surface of heterogeneous catalysts using modern spectroscopic methods is complicated by the fact that the hydrocarbon molecules contain only carbon and hydrogen atoms the spectra of which are often difficult to interpret unambiguously. The problem is solved by analyzing the results obtained using various methods of surface studies, such as temperature-programmed desorption, high-resolution X-ray photoelectron spectroscopy, IR reflection absorption spectroscopy and near-edge X-ray absorption fine structure (NEXAFS) spectroscopy. For instance, a NEXAFS study of methylcyclohexane ($C_6H_{11}CH_3$) dehydrogenation reported by Gleichweit [111] revealed that most part of $C_6H_{11}CH_3$ molecules are desorbed from the Pt(111) surface during the reaction while the remaining methylcyclohexane (35 %–45%) is converted into a π-allylic compound ($C_6H_8CH_3$). It was assumed that the π-allylic ring is formed due to adsorption of a methylcyclohexane molecule on the catalyst surface involving three carbon atoms. As the temperature increases, the π-allyl undergoes dehydrogenation to benzyl with elimination of hydrogen from the methylene unit ($C_6H_5CH_2$) followed by the formation of toluene ($C_6H_5CH_3$). According to NEXAFS data, the methylcyclohexane and toluene molecules are in-plane with the Pt(111) surface, whereas the benzyl structure has a nearly normal orientation.[133]

Similar results were obtained in a study on dehydrogenation of dicyclohexylmethane (in this molecule, adjacent hydrocarbon rings are connected through a methylene unit). As a consequence, the diphenylmethane–dicyclohexylmethane pair is characterized by a storage capacity of 6.66 mass % H_2, which is higher than that of the toluene–methylcyclohexane system. However, diphenylmethane ($C_6H_5–CH_2–C_6H_5$) and dicyclohexylmethane ($C_6H_{11}–CH_2–C_6H_{11}$) are liquids at temperatures below 30°C. Exhaustive hydrogenation of diphenylmethane to dicyclohexylmethane proceeds quite efficiently on the 5% Ru/C catalyst at 120 °C and a hydrogen pressure of 10 MPa. A NEXAFS study showed that dicyclohexylmethane dehydrogenation on the Pt(111) surface involves the formation of an intermediate containing two π-allylic moieties (Scheme 5).[134] This compound is formed through adsorption of dicyclohexylmethane on the catalyst surface involving a total of six hydrogen atoms (three H atoms from each of the two hydrocarbon rings). Then, about 30% of the substrate are desorbed, while the remaining amount is dehydrogenated *via* transformation of one π-allylic species to the phenyl group and associative desorption of hydrogen.[135] Raising the temperature causes dehydrogenation of the second π-allylic species to give diphenylmethane.

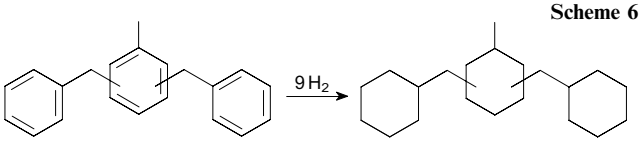
Based on the NEXAFS spectral patterns and peak intensity ratios, it was found that the phenyl group just formed is tilted to the catalyst surface. Both C–H bonds in the methylene unit dissociate; the process is accelerated with increasing temperature, which leads to carbonization of the catalyst surface and degradation of the starting dicyclohexylmethane as a hydrogen carrier. Dehydrogenation of dicyclohexylmethane on the Pd(111) surface instead of Pt(111) proceeds without formation of the π-allylic species containing one phenyl group. This favours the decrease in the temperature of formation of diphenylmethane; however, the C–H bonds also dissociate at lower temperatures, which leads to rapid degradation of the starting dicyclohexylmethane.[135]

In addition to the hydrogen storage systems with two liquid substrates, the so-called liquid organic hydrogen carriers (LOHC) concept is widely used. It is based on the assumption that only the hydrogen carrier is in the liquid state. This allowed one to considerably increase the number of systems treated as potential candidates for hydrogen storage. In particular, there has been considerable recent interest in low-melting compounds (and their mixtures), such as benzyltoluene ($C_{14}H_{14}$) and dibenzyltoluene ($C_{21}H_{21}$) that are used as heat transfer fluids Marlotherm, Farolin and Diphil; they are characterized by high purity, thermal stability and long operating life.[136–141] The storage capacity of systems based on these compounds is 6.2 mass % H_2. This value is intermediate between the storage capacities of toluene and diphenylmethane. The viscosity of benzyltoluene is lower than that of dibenzyltoluene, but the latter has a lower saturated vapour pressure, which is of importance for carrying out reversible reactions.[139, 140] Dibenzyltoluene is a liquid under normal conditions. The enthalpy of hydrogenation of benzyltoluene and dibenzyltoluene is 63.5 and 65.4 kJ mol^{-1} per mole of H_2, respectively; this is closer to the calculated value

(62.8 kJ mol^{-1})[95] rather than the corresponding values for toluene (67.4 kJ mol^{-1}) and benzene (68.6 kJ mol^{-1}). Therefore, hydrogen release in the dehydrogenation of both perhydrobenzyltoluenes is possible at lower temperatures compared to the two last-mentioned monocyclic compounds.

The hydrogenation reactions of benzyltoluene and dibenzyltoluene (Scheme 6) proceed under identical conditions. The highest efficiency is attained on Ru catalysts at 180°C and hydrogen pressures in the range from 20 to 50 atm; however, the rate of the reaction involving dibenzyltoluene is somewhat lower.[138]

Scheme 6



A possible cause of slowing down the reaction is the formation of numerous intermediate half-hydrogenated products, so their hydrogenations follow different pathways and proceed at different rates. These processes result in a mixture of perhydrodibenzyltoluene isomers having spatial conformers that negatively affect the volume of hydrogen released and the rate of hydrogen release in the dehydrogenation. The kinetics of the hydrogenation reaction is significantly improved using a mixture of dibenzyltoluene and toluene and the efficiency of the process reaches a maximum value at a dibenzyltoluene/toluene ratio of three. However, a 100% conversion takes a long time. As a consequence, in spite of low enthalpy of hydrogenation, the results of hydrogenation and dehydrogenation obtained using benzyltoluene- and dibenzyltoluene-based systems are poorer than the results obtained using the systems based on benzene and toluene.

According to quantum chemical calculations,[95] the standard enthalpies of hydrogenation of fused compounds with alternating benzene rings and π-conjugated five-membered nitrogen-containing rings are lower than those of compounds containing other types of ring combinations. The hydrogen storage capacity of carbazole is 7.19 mass %. This feature, as well as the fact that the hydrogen uptake and release temperatures of carbazole are lower than those of carbocyclic hydrocarbons inspired great optimism regarding the use of heterocyclic compounds as a basis for chemical hydrogen storage systems. However, further studies showed that reversible hydrogenation–dehydrogenation reactions of carbazole-based systems are slow.[142,143] The ring containing the heteroatom is readily hydrogenated even at temperatures below 150 °C. The stability of carbazoles towards ring-opening reactions increases if the heteroatom is shielded by alkyl substituents. At the same time, the presence of an additional alkyl group leads to a decrease in the storage capacity by 0.4 mass % H_2 per methylene unit since the substituent is not involved in the uptake and release of H_2.

The molecule of *N*-ethylcarbazole characterized by a storage capacity of 6.79 mass % H_2 seems to be optimum for hydrogen storage systems; elongation of the alkyl chain by more than two carbon atoms appeared to be inappropriate. It should be noted that hydrogenation of *N*-ethylcarbazole and dehydrogenation of perhydro-*N*-ethylcarbazole begins at relatively low temperatures and the initial reaction rate is rather high; however, the reactions subsequently slow down owing to steric hindrance associated with the formation of intermediates, just as in the case of the reactions involving carbazole.[144–147] This is possibly due to dealkylation of *N*-ethylcarbazole at the C–N bond to give carbazole and hydrocarbon fragments that are adsorbed on the catalyst surface. One more cause is the fact that perhydro-*N*-alkylcarbazole has at least five spatial isomers in the equilibrium state.[148] Structural features and different physicochemical characteristics of the isomers increase the number of the dehydrogenation reaction pathways, which also influences the reaction kinetics and, correspondingly, the volume and release rate of hydrogen. Taking account of low hydrogen storage capacity of substituted carbazole homologues, their potential as a basis for a system for storage and release of chemically pure hydrogen is lower compared to corresponding carbocyclic hydrocarbons. Large-scale synthesis of unsaturated products of specified purity is difficult, in particular, when distilling coal tar resin.[149,150]

3.2.3. Systems based on fused compounds

A distinctive feature of fused hydrocarbons is the chemical bond between adjacent rings. The simplest hydrogen storage system based on fused compounds is the naphthalene–decalin pair characterized by a hydrogen storage capacity of 7.25 mass %, which is higher than that of monocyclic systems. However, unlike benzene and toluene, naphthalene ($C_{10}H_8$) is a solid under normal conditions.

In the naphthalene molecule, two equivalent rings form a labile aromatic system including 10 π-electrons.[103–105] The bridgehead atoms C(9) and C(10) share one π-electron between three C–C bonds each, while all other carbon atoms contribute one π-electron to two π-bonds; therefore, the π-bond between the C(9) and C(10) atoms is weaker than all other bonds. Redistribution of the π-electron density is responsible for the larger number of unused valencies of the C(1), C(4), C(5) and C(8) atoms. Symmetry violation leads to changes in the bond lengths and bond angles and to a decrease in the stabilization energy of the naphthalene molecule to 256 kJ mol^{-1}.[103] A comparison with the stabilization energy of benzene showed that hydrogenation of the first unsaturated ring of naphthalene requires only ~105 kJ mol^{-1}; this is responsible for the higher reactivity of naphthalene in the hydrogenation reaction and for successive character of saturation of the hydrocarbon rings with hydrogen.

The hydrogenation of naphthalene on platinum[151] and nickel[152] catalysts (Scheme 7) involves the following stages:

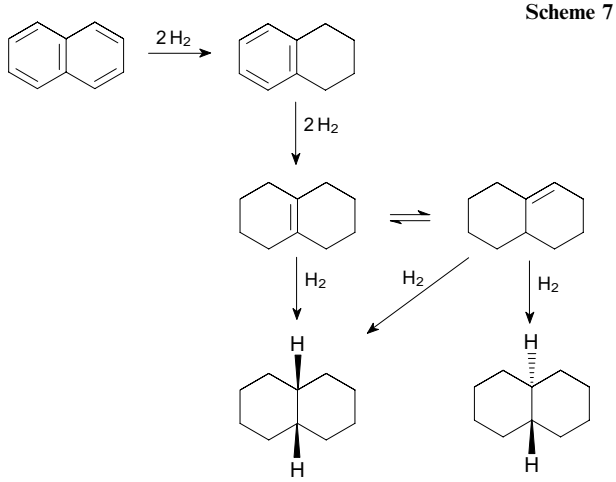
— *cis*-addition of two dissociatively adsorbed hydrogen atoms to give tetralin (1,2,3,4-tetrahydronaphthalene);

— the formation of tetralin surface complexes with active sites of the catalyst; and

— hydrogenation to 9,10-octalin.

Unsaturated rings of the naphthalene and tetralin molecules are adsorbed in the form of a transient π–σ-complex which is in equilibrium with the π- and σ-complexes. The transient π–σ- and π-forms are associative, whereas the σ-form is dissociative.[153,154] The adsorption of naphthalene occurs on a single active site, while that of tetralin requires a group of active metal atoms. Consequently, the hydrogenation of tetralin is a structure-sensitive reaction, while that of naphthalene is not. However, opinions are still different as to this issue. A comparison of the data obtained in different conditions showed that the predominant form of adsorption

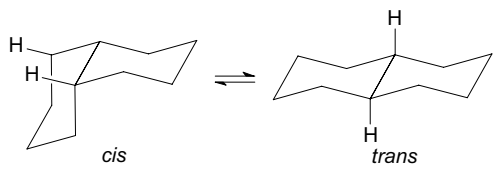
Scheme 7



and the reaction pathway depends on the properties of the catalyst (nature of the active component and substrate, as well as the method of preparation and subsequent pretreatment of the catalyst) and on the reaction conditions (temperature, hydrogen pressure and reactant concentrations). For instance, depending on the reaction conditions, 9,10-octalin is either hydrogenated to *cis*-decalin or undergoes isomerization to octahydronaphthalene (1,9-octalin) which is in turn hydrogenated to *cis*- and *trans*-decalin. The *cis*-to-*trans*-decalin ratio depends on the orientation (towards or outwards the surface) of the hydrogen atom in position 10 in the intermediate octahydronaphthalene during the formation of decalin.[151,155] A 100% conversion of naphthalene to intermediate tetralin on the classical heterogeneous catalyst Pd/C in the presence of ionic liquid occurs at a hydrogen pressure of 1 atm; however, the final product, decalin, is not formed under these conditions.[156]

The molecule of decalin ($C_{10}H_{18}$) contains two fused cyclohexane rings, each being 1,2-disubstituted relative to the other. The optically inactive molecule of *trans*-decalin has a centre of symmetry at the midpoint of the line connecting the C(9) and C(10) atoms. The asymmetric (chiral) *cis*-decalin molecule, undergoes ring inversion; as a result, two interconvertible chair conformations are mirror images of each other[103–105] and therefore *cis*-decalin exists as a non-resolvable (±) pair. The structural conformations of *cis*- and *trans*-decalin molecules are shown in Scheme 8.

Scheme 8



Like the dehydrogenation of cyclohexane, that of decalin is most efficiently catalyzed by Pt-based catalysts.[92] The main feature of the latter process is that decalin has spatial isomers and the reaction proceeds as independent dehydrogenations of its *cis*- and *trans*-isomers that can undergo *cis*–*trans* isomerization. Such a competitive character of the process significantly influences the reaction kinetics.[157] The kinetics of decalin dehydrogenation on the Pt catalysts supported on γ-Al_2O_3, SiO_2 or activated carbon in the temperature range of 275–345 °C was described in terms of the Hougen–Watson model with inclusion of adsorption of the various components of the reaction mixture.[158]

A comparison of Pt catalysts supported on various carbon substrates revealed the following facts: catalysts supported on ordered mesoporous carbon are more preferred in the initial stages of decalin dehydrogenation, while catalysts supported on carbon substrates with large pores (*e.g.*, carbon black) are more efficient in the case of long-term operation.[159] In both cases, the stability of operation is associated, with lower degree of carbonization of the catalyst and weaker blockage of a proportion of platinum in the support micropores.[160] These features also underlie the advantage of carbon supports over oxide ones that contain acidic sites facilitating cleavage of chemical bonds.[161] Considering the rate of hydrogen release in identical reaction conditions, monocyclic cyclohexane and methylcyclohexane are more preferred than bicyclic decalin.[162]

Kariya *et al.*[107] contributed largely to the study of decalin dehydrogenation. Namely, they showed that reactions in the presence of carbon-supported catalysts proceed faster compared to on any other supports. However, no strict correlation between the reaction rate and the nature of the carbon material was found, although differences in the particle size, pore size and specific surface areas of different carbon supports are reflected in the reaction rate. Raising the temperature caused the rate of reactions on all catalysts to increase; this was explained by weak adsorption of aromatic compounds formed during the dehydrogenation on the catalyst surface. The reaction rate was increased by creating a high gradient at the catalyst/support interface owing to different rates of evaporation and deposition of liquid substrate droplets on the catalyst surface. This approach gave an impetus to numerous studies.

Hodoshima *et al.*[163] experimentally studied the dehydrogenation of decalin and tetralin and found that the reaction rate increases as adsorbed hydrogen is continuously removed from the catalyst surface. The state of the substrate under boiling, distillation and refluxing conditions is intermediate between gaseous and liquid. It was called a 'liquid film'. The thin 'liquid film' is superheated in the course of liquid-phase dehydrogenation, which favours the occurrence of the endothermic reaction. Hydrogen gas ease diffuses through the thin organic liquid film without bubbling. Distillation of aromatic products causes slowing down the adsorption and carbonization of the catalyst, which is often observed under liquid-phase reaction conditions at high temperatures. In the 'liquid film' state, a 90% conversion of decalin is attained at 265 °C, the reaction rate being high at 240 °C.

Using decalin and tetralin as substrates, Hodoshima *et al.*[163] found that, as in the experiments with cyclohexane, physical mixing of the Pt/C and Pd/C catalysts as well as the addition of the second metal to platinum favours acceleration of the dehydrogenation of decalin and tetralin compared to the reaction on the single-component Pt/C catalyst. In particular, a 100% conversion of both decalin isomers was achieved on the Pt–Re/C catalyst. The rate of the complete conversion of decalin into naphthalene appeared to be sensitive to the initial decalin/catalyst ratio. The maximum reaction rate was observed at a decalin : catalyst ratio of 3.3 mL g^{-1}. The optimum decalin : catalyst ratio is different for different types of reactors.[164]

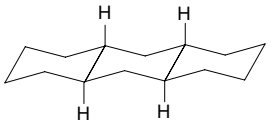
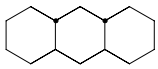
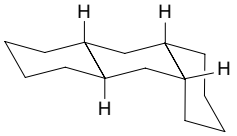
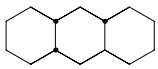
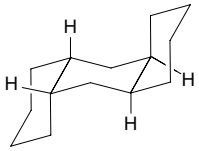
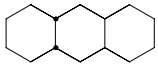
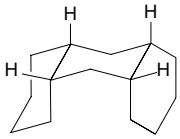
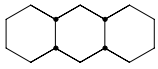
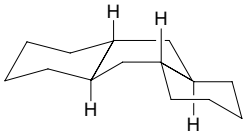
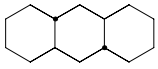
A comparative study[165] was aimed at testing Pt/C catalysts prepared by impregnation, deposition, ion

exchange and a polyol method. It was shown that the catalysts prepared by the last-mentioned two methods provided higher conversion of decalin and higher hydrogen release rate than the catalysts prepared using conventional methods (impregnation and deposition). These results were obtained using highly dispersed platinum particles. It was found [166] that the activity of catalysts can be improved by controlling pH values when the active metal species are immobilized on the support and by abruptly raising the temperature when reducing the catalyst. An increase in the platinum content causes the reverse effect since the Pt particles are coarsened and a certain proportion of active platinum sites becomes less accessible to the reaction.[167] Yet another factor is partial blockage of platinum in micropores owing to adsorption of naphthalene. This problem is solved by, *e.g.*, changing the design of the catalytic reactor in order to provide faster removal of hydrogen. This favours partial removal of naphthalene and other reaction products and causes deblocking of the active sites of the catalyst.

The molecule of the second representative of fused compounds, anthracene ($C_{14}H_{10}$), comprises three coplanar unsaturated rings. The theoretical storage capacity of the anthracene–perhydroanthracene ($C_{14}H_{24}$) system is 7.27 mass % H_2. Three fused rings in the anthracene molecule form a labile aromatic system including 14 π-electrons.[103–105] Owing to the effect of two outer rings on the central one, the molecular deformation is more pronounced compared to the naphthalene molecule and the electron density is respectively redistributed in such a manner that the central atoms, C(9) and C(10), acquire the properties of reaction centres. The stabilization energy of the anthracene molecule is 350 kJ mol^{-1}.[103] That is why the energy of hydrogenation of the central unsaturated ring in this molecule is low, *viz.*, 48 kJ mol^{-1}. Higher reactivity of anthracene in the hydrogenation reaction as compared to naphthalene and benzene is due to considerable stabilization energy differences between these compounds. Indeed, high conversion of anthracene into dihydroanthracene on the $Cu-Cr_2O_3$ catalyst is attained at 100 °C and a pressure of 95 atm.[104] However, deeper hydrogenation requires higher temperatures (240–280 °C).[168] The hydrogenation of naphthalene on Pt catalysts supported on microporous zeolite ZSM-5 or mixed oxides TiO_2-ZrO_2 in the temperature range of 250–300 °C is characterized by more than 97% selectivity with respect to decalin,[169] whereas anthracene hydrogenation under identical conditions proceeded with a tenfold lower selectivity with respect to perhydroanthracene. This is due to neglect of the stabilization energy difference between naphthalene and benzene and strengthening of diffusion limitations owing to the larger size of the anthracene molecule compared to the naphthalene molecule.

A 100% conversion of anthracene into a mixture of intermediates including 9,10-dihydroanthracene ($C_{14}H_{12}$),

Table 1. Selected physicochemical properties of perhydroanthracene isomers and their content in the hydrogenation product of anthracene.[105, 178, 179]

No.	Isomers			T/°C		ΔH /kJ mol^{-1} (see [c])	C /mass % (see [d])
	configuration [a]	conformation	structural formula [b]	melting point	boiling point		
1	*trans-cisoid-trans* (*trans-syn-trans*; tst)			90	272–273	0	9.9
2	*trans-cisoid-cis* (*cis-transoid-trans*; *cis-trans*; ct)			40	274–275	11.0	0.9
3	*cis-transoid-cis* (*cis-anti-cis*; cac)			122	–	23.3	55.8
4	*cis-cisoid-cis* (*cis-syn-cis*; csc)			61	282–283	34.0	23.8
5	*trans-transoid-trans* (*trans-anti-trans*; tat)			49–50	–	24.5	9.6

[a] Listed are actual and old (in parentheses) terms for configurations. [b] For ring junction points, solid circles denote hydrogen atoms above the ring plane; otherwise, hydrogen atoms are below the ring plane. [c] Given are the enthalpies of formation calculated relative to isomer *1*. [d] Content in the product.

1,2,3,4-tetrahydroanthracene ($C_{14}H_{14}$) and *sym*-octahydroanthracene ($C_{14}H_{18}$) on a Ni-containing zeolite catalyst in supercritical CO_2 was achieved at 100 °C and a pressure of 69 atm.[170] Anthracene conversion into 1,2,3,4,5,6,7,8-octahydroanthracene with more than 60% selectivity on catalysts based on Pd and Rh nanoparticles entrapped in a silica sol–gel matrix was observed at 80 °C and a hydrogen pressure of 28 atm.[171] The hydrogenation of anthracene to 9,10-dihydroanthracene on rhodium and iridium nanoparticles entrapped in aluminium oxyhydroxide nanofibres[172] was performed at room temperature and a hydrogen pressure of 1 atm. However, conversion into other products required more severe reaction conditions and a higher concentration of the active component (10%). The reaction on ruthenium nanoparticles (30 °C, a pressure of 20 atm, duration 16 h) afforded *sym*-octahydroanthracene (90%) and perhydroanthracene (10%) as major products.[173] The capability of activated carbon to split H_2 to atomic hydrogen and to transfer hydrogen atoms to the aromatic ring was reported.[174] However, anthracene hydrogenation at 300°C on such nonmetallic catalysts produces nearly equal amounts of dihydro-, tetrahydro- and octahydroanthracenes while no perhydroanthracene was found.[175] The yield of the final product of anthracene hydrogenation on the classical Pd/C catalyst at 300 °C and a hydrogen pressure of 30 atm was at most 25%.[176] Anthracene hydrogenation on catalysts based on 10% Pd-substituted polyoxometalate having a Keggin structure, supported on γ-alumina and activated carbon (230°C, a hydrogen pressure of 30 atm, duration 1 h) demonstrated a 93% selectivity with respect to perhydroanthracene.[177]

The hydrogenation of anthracene on the 3% Pt/C catalyst (C is Sibunit, 280 °C, hydrogen pressure of 90 atm, duration nearly 40 h) was characterized by 100% conversion giving five perhydroanthracene isomers.[178, 179] The chemical composition, structures and selected physicochemical characteristics of the isomers are listed in Table 1. The most stable isomer *1* has the *trans-cisoid-trans* configuration; the enthalpies of formation of other conformations calculated relative to that of *1* are higher. Two isomers are unstable, *viz*., the instability of isomer *5* is due to the presence of a forced boat conformation of the central cyclohexane moiety, while isomer *4* is unstable owing to *syn*-axial methylene interaction.[105]

A comparison of experimental data with the results of theoretical calculations of formation and consumption of the intermediate and final products made it possible to propose the following sequence of transformations in the anthracene hydrogenation reaction (Scheme 9).

Dehydrogenation of the mixture of isomers involves a relatively fast conversion of the less stable isomers into the target products followed by the dehydrogenation of the most stable isomer *1* at high temperatures (> 400 °C) affording cracking and hydrogenolysis products.

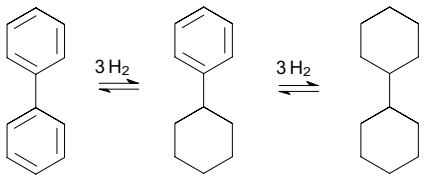
3.2.4. Systems based on hydrocarbons with linearly connected rings

Systems based on hydrocarbons with linearly connected rings demonstrate to some extent independent behaviour of adjacent rings. The simplest system in question is the biphenyl–bicyclohexyl pair characterized by a storage capacity of 7.23 mass % H_2, which is comparable with that of the naphthalene–decalin system. However, the former pair has been studied much poorer than the latter, probably, since (i) biphenyl ($C_{12}H_{10}$) and bicyclohexyl ($C_{12}H_{22}$) are not easily commercially available and (ii) there are thermodynamic limitations on the hydrogenation reaction. The stabilization energy of the most stable conformation of the biphenyl molecule is 330 kJ mol^{-1},[103–105] which implies a considerable increase in the energy consumption for hydrogenation of one unsaturated ring in the biphenyl molecule as compared to not only naphthalene, but also benzene.

Biphenyl is a solid under normal conditions. Each of the two isolated rings of this molecule has its own six π-electron aromatic system. The formation of a common π-electron cloud seems to be energetically unfavourable. In the solid state, the biphenyl molecule retains its high symmetry, whereas in the gas phase, mutual repulsion between hydrogen atoms in positions 2 and 2′ causes the ring planes to arrange at an angle of ~45°; this angle increases if the hydrogens in positions 2 and 2′ are replaced by methyl groups.[180, 181]

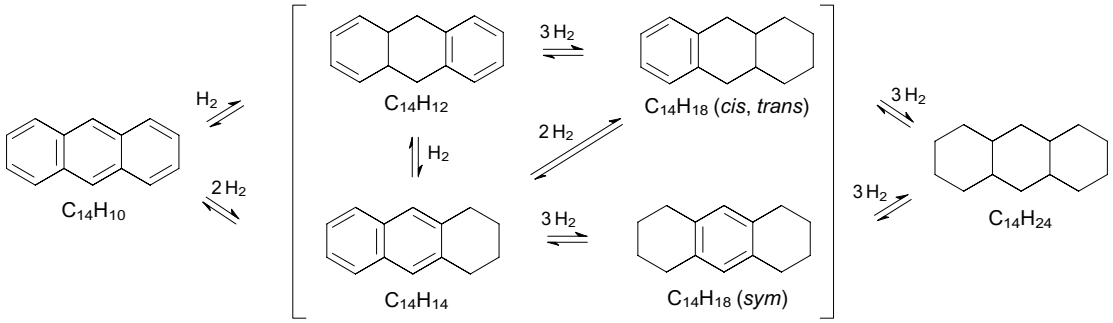
Hydrogenation of biphenyl on Pt, Pd or mixed Pt–Pd-catalysts proceeds without significant difficulties (Scheme 10).

Scheme 10



The initial rate of biphenyl hydrogenation on the 3 mass % Pt/C catalyst is lower than that of naphthalene hydrogenation on the same catalyst, which is consistent with the difference between corresponding stabilization energies. However, conversion of intermediate cyclohexylbenzene into bicyclohexyl proceeds faster than conversion of tetralin into decalin.[157, 181] Probably, the electron density distribution in the tetralin molecule better resembles that in the benzene rather than naphthalene molecule, which

Scheme 9



decreases the overall rate of naphthalene hydrogenation in the case of much stronger steric hindrance due to non-coplanarity and low accessibility of the bridgehead carbon atoms. Contrary to this, the degree of delocalization of the positive charge of the σ-complex of cyclohexylbenzene is higher than in the unsubstituted π-complex of benzene, which favours acceleration of the hydrogenation reaction as compared to the hydrogenation of tetralin, especially at *meta*- and *para*-positions.

The results obtained in a study[180] on the biphenyl hydrogenation reaction were described using the pseudo-first order kinetic equation since the biphenyl adsorption rate is incomparable with the rate of dissociative adsorption of hydrogen. It was found that biphenyl is adsorbed on the catalyst surface five times faster than cyclohexylbenzene.

The energy barrier to internal rotation around the C–C axis in the bicyclohexyl molecule is low, and both rings execute free rotation relative to each other.[182] Since there is no high torsional strain, the angles and bond lengths in this molecule remain close to the corresponding values for the cyclohexane molecule. Similarly to the dehydrogenation of cyclohexane, that of bicyclohexyl most efficiently proceeds on Pt and Pd catalysts at temperatures above 250 °C. The temperature dependences of conversion of these compounds upon dehydrogenation on the 3 mass % Pt/C catalyst behave in a symbate manner.[183] At 320 °C, the conversion of bicyclohexyl is 99.9% and the selectivity with respect to biphenyl is 97.6%, being higher than the corresponding values for decalin in spite of a less favourable ratio of the enthalpies of reaction. For instance, the enthalpy of 100% conversion of bicyclohexyl is 399.5 kJ mol^{-1} (calculated with respect to biphenyl) while the enthalpy of exhaustive *cis*-decalin dehydrogenation is 320.1 kJ mol^{-1} (calculated with respect to naphthalene).[95] Such a large difference apparently is due to different orientations of the decalin steric isomers relative to the same active sites, whereas bicyclohexyl has no steric isomers.

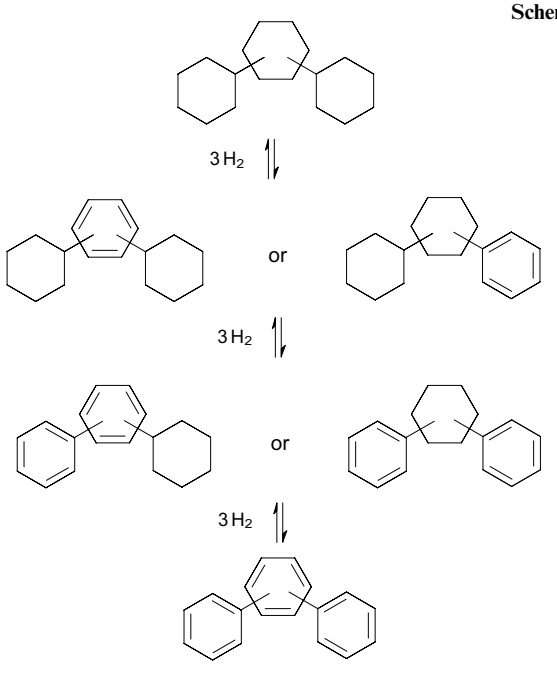
The main difference between tricyclic hydrocarbon terphenyl ($C_{18}H_{14}$) and biphenyl consists in that the former has three isomers (*ortho*-, *meta*- and *para*-). Although these isomers are structurally different and have different physicochemical properties, they are characterized by the same hydrogen storage capacity (7.26 mass %). Phenyl groups as substituents are strong σ-donors and cause the bond angle at carbon atoms in the benzene ring to decrease from its conventional value of 120°.[118] Like in the case of the biphenyl molecule, deformation of σ-bonds in the benzene rings makes the formation of a common π-electron cloud energetically unfavourable. All rings in the terphenyl molecule behave to some extent independently; however, different arrangement of phenyl groups leads to the situation where the outer rings are rotated relative to the central ring, which hampers in-plane adsorption of molecules on the catalyst surface.[184]

As in the case of systems based on toluene derivatives, the sources of substrates include commercially available heat transfer fluids based on a mixture of terphenyl isomers (*e.g.*, Therminol-72, Dowtherm HT, Delowax, Santowax) that exhibit good thermal physical properties and have low saturated vapour pressure. Kustov *et al.*[89] proposed to take account of high boiling points of terphenyl isomers in developing corresponding hydrogen storage systems. For instance, if the boiling point of the substrate being dehydrogenated is higher than the reaction temperature, liquid-phase catalytic dehydrogenation on Pt or Pd catalysts proceeds more selectively and efficiently than on traditional catalysts for dehydrogenation. Since the dehydrogenation reaction is endothermic, no overheating is allowed; this decreases the probability of catalyst deactivation and coking. Hydrogen freely diffuses in the gas phase through a thin 'liquid film' of organic hydrogen-containing compounds.

Hydrogenation of terphenyl isomers proceeds most efficiently on catalysts containing noble metals (Pt, Pd, *etc.*) in the temperature range of 120–200 °C at a hydrogen pressure of 70 atm. Dehydrogenation of corresponding perhydroterphenyl isomers is carried out in the temperature range of 250–340 °C.[185] Under particular conditions all the three perhydroterphenyl isomers can undergo interconversions of *cis*-conformers to *trans*-ones, while the *ortho*-isomer can also isomerize to *meta*- and *para*-isomers. However, since the central hydrocarbon ring in the three perhydroterphenyl isomers adopts a *twist*-conformation, configurations of their *cis*- and *trans*-isomers look alike. This underlies similarity in the behaviour of different *cis*- and *trans*-forms of the *ortho*-, *meta*- and *para*-perhydroterphenyl isomers in the temperature range from 260 to 340 °C; as a consequence, isomerization has no strong impact on the rate of hydrogen release, as in the dehydrogenation of decalin. Dehydrogenation of the *ortho*-, *meta*- and *para*-perhydroterphenyl isomers (Scheme 11), as well as hydrogenation of corresponding terphenyl isomers mainly proceeds at the outer rings. This can be due to the formation of π-allylic species, as in the dehydrogenation of methylcyclohexane.

However, this is not the main mechanism because the number of intermediate products increases as the central ring in the perhydroterphenyl isomers becomes more accessible. At the same time, an increase in the number of dehydrogenation pathways of the perhydroterphenyl isomers causes the formation of a larger number of intermediates, which slows down the reaction as compared to the dehydrogenation of bicyclohexyl.[185–188]

Scheme 11



4. Conclusion

From the aforesaid it follows that only physical methods of accumulation and storage of hydrogen (as cryogenic liquid or in compressed state in high-pressure tanks) and subsequent release of the substance can be considered technologically developed. Methods for hydrogen storage in metal hydrides, adsorption materials and their modifications and in the chemically bound state are in the early stage of development and none of them is fundamentally superior to all other approaches.

Hydrogen is a constituent of organic matter; therefore, its density and abundance are independent of external factors. Hydrogen present in organic compounds can be safely stored and transported over long distances under normal conditions. This provides an exclusive advantage to chemical systems since all other systems should meet specific requirements on temperature, pressure and air-tightness. In this review we integrate and summarize the results of studies on exhaustive hydrogenation and dehydrogenation of differently fused polycyclic hydrocarbons in the presence of heterogeneous catalysts. We showed that competing reactions influencing the hydrogenation–dehydrogenation process cyclicity proceed even in such relatively simple systems as bi- and tricyclic hydrocarbons. Taking into account the structural features of steric isomers, polycyclic hydrocarbons with linearly connected rings are more advantageous than fused compounds with respect to both the rate of full substrate saturation with hydrogen and the amount and release rate of hydrogen evolved in the dehydrogenation reaction.

Clearly, research in this field will be aimed at enhancing activity and improving selectivity of heterogeneous catalysts, first of all, through reducing the content of noble metals by combining them with other elements including non-noble metals and through the design of hierarchical catalytic systems.

References

1. M.S.Dresselhaus, I.L.Thomas. *Nature (London)*, **414**, 332 (2001)
2. A.Zuttel. *Mater. Today*, **9**, 24 (2003)
3. J.M.Tour, C.Kittrell, V.L.Colvin. *Nat. Mater.*, **9**, 871 (2010)
4. S.Shafiee, E.Topal. *Energy Policy*, **37**, 181 (2009)
5. M.Balat, H.Balat. *Appl. Energy*, **86**, 2273 (2009)
6. J.Ren, N.M.Musyoka, H.W.Langmi, M.Mathe, S.Liao. *Int. J. Hydrogen Energy*, **42**, 289 (2017)
7. R.B.Biniwale, S.Rayalu, S.Devotta, M.Ichikawa. *Int. J. Hydrogen Energy*, **33**, 360 (2008)
8. V.S.Arutyunov, G.V.Lisichkin. *Russ. Chem. Rev.*, **86**, 777 (2017)
9. B.N.Kuzyk, Yu.V.Yakovets. *Rossiya: Strategiya Perekhoda k Vodorodnoy Energetike*. (Russia: Strategy of Transition to Hydrogen Energy). (Moscow: Institute for Economic Strategies, 2007)
10. V.S.Arutuynov. *Russ. Chem. Rev.*, **61**, 1140 (1992)
11. P.E.Dodds, I.Staffell, A.D.Hawkes, F.Li, P.Grünewald, P.Ekins. *Int. J. Hydrogen Energy*, **40**, 2065 (2015)
12. A.B.Yaroslavtsev, Ju.A.Dobrovolsky, N.S.Schaglaeva, L.A.Frolova, E.V.Gerasimova, E.A.Sanginov. *Russ. Chem. Rev.*, **81**, 191 (2012)
13. J.Celorrio, R.Florez-Montano, E.Moliner, M.J.Pastor. *Int. J. Hydrogen Energy*, **39**, 5371 (2014)
14. S.G.Chalk, J.F.Miller. *J. Power Sources*, **159**, 73 (2006)
15. H.L.Hellman, R.Van den Hoed. *Int. J. Hydrogen Energy*, **32**, 305 (2007)
16. S.S.Ivanchev, S.V.Myakin. *Russ. Chem. Rev.*, **79**, 117 (2010)
17. S.Satyapal, J.Petrovic, C.Read, G.Thomas, G.Ordaz. *Catal. Today*, **120**, 246 (2007)
18. P.T.Aakko-Saksa, Ch.Cook, J.Kiviaho, T.Repo. *J. Power Sources*, **396**, 803 (2018)
19. A.T.Wijayanta, T.Oda, Ch.W.Purnomo, T.Kashiwagi, M.Aziz. *Int. J. Hydrogen Energy*, **44**, 15026 (2019)
20. M.Kaur, K.Pal. *J. Energy Storage*, **23**, 234 (2019)
21. E.Rivard, M.Trudeu, K.Zaghib. *Materials*, **12**, 1973 (2019)
22. I.Streedhar, K.M.Kamani, B.M.Kamani, B.M.Reddy, A.Venugopal. *Renew. Sust. Energy Rev.,* **91**, 838 (2018)
23. A.M.Abdalla, Sh.Hossain, O.B.Nisfindy, A.T.Azad, M.Dawood, A.K.Azad. *Energy Convers. Manag.*, **165**, 602 (2018)
24. P.Preuster, C.Papp, P.Wasserscheid. *Acc. Chem. Res.*, **50**, 74 (2017)
25. T.Rude, A.Bosmann, P.Preuster, P.Wasserscheid, W.Arlt, K.Muller. *Energy Technol.*, **6**, 529 (2018)
26. T.Shimbayashi, K.Fujita. *Tetrahedron*, **76**, 130946 (2020)
27. M.Feller. *Phys. Sci. Rev.*, (2018); DOI: 10.1515/psr-2018-0033
28. *DOE Hydrogen and Fuel Cells Program*; www.hydrogen.energy.gov (accessed 4 July 2020)
29. J.Yang, A.Sudik, C.Wolverton, D.J.Siegel. *Chem. Soc. Rev.*, **39**, 656 (2010).
30. R.S. Irani. *MRS Bull.*, **9**, 680 (2002)
31. B.P.Tarasov, V.V.Burnascheva,M.V.Lototsky, V.A.Yartys. *ISJAEE*, (12), 14 (2005)
32. A.F.Chabak, A.I.Ulianov. *Russ. Engen. Res.*, (4), 48 (2007)
33. N.K.Zhevago, V.I.Glebov, E.I.Denisov, S.V.Koroptsev, A.F.Chabak. *ISJAEE*, (9), 106 (2012)
34. J.Wolf. *MRS Bull.*, **9**, 684 (2002)
35. R.O.Stroman, M.W.Schuette, K.Swider-Lyons, J.A.Rodgers, D.J.Edwards. *Int. J. Hydrogen Energy*, **39**, 11279 (2014)
36. R.Strobel, J.Garche, P.T.Moseley, L.Jorissen, G.Wolf. *J. Power Sources*, **159**, 781 (2006)
37. O.V.Krylov. *Geterogennyi Katalyz*. (Heterogeneous Catalysis). (Moscow: Akademkniga, 2004)
38. H.W.Langmi, A.Walton, M.M.Al-Mamouri, S.R.Johnson. *J. Alloys Compd.*, **356–357**, 710 (2003)
39. D.Scarano, S.Bordiga, C.Lamberty, G.Ricchiardi, S.Bertarione, G.Spoto. *Appl. Catal. A: Gen.*, **307**, 3 (2006)
40. D.J.Durbin, A.Malardier-Jugroot. *Int. J. Hydrogen Energy*, **38**, 14595 (2013)
41. P.Jena. *J. Phys. Chem. Lett.*, **2**, 206 (2011)
42. D.S.Su, G.Centi. *J. Energy Chem.*, **22**, 151 (2013)
43. B.V.Fenelonov, E.A.Ustinov, V.A.Yakovlev, Ch.N.Barnakov, M.S.Melgunov. *Kinet. Katal.*, **48**, 599 (2007)
44. P.M.Eletskii, V.A.Yakovlev, V.B.Fenelonov, V.N.Parmon. *Kinet. Katal.*, **49**, 708 (2008)
45. B.Panella, M.J.Hirsher. *J. Alloys Compd.*, **404–406**, 399 (2005)
46. M.Marella, M.Tomaselli. *Carbon*, **44**, 1404 (2006)
47. J.W.Patrick, A.Arenillas, W.Shi, C.E.Snape. *Carbon*, **44**, 1376 (2006)

48. E.Poirier, R.Chaine, P.Bernard, D.Cassement, L.Lafi, E.Melanson, T.K.Bose, S.Desilets. *Appl. Phys. A*, **78**, 961 (2004)
49. T.Heine, L.Zechkov, G.Seifert. *Phys. Chem. Chem. Phys.*, **6**, 980 (2004)
50. P.X.Hou, S.T.Xu, Z.Ying, Q.H.Yang, C.Liu, H.M.Cheng. *Carbon*, **41**, 2471 (2003)
51. V.Jain, B.Kandasubramanian. *J. Mater. Sci.*, **55**, 1865 (2020)
52. A.Yu.Tsivadze, O.E.Aksyutin, A.G.Ishkov, M.K.Knyazeva, O.V.Solovtsova, I.E.Men'shchikov, A.A.Fomkin, A.V.Shkolin, E.V.Khozina, V.A.Grachev. *Russ. Chem. Rev.*, **88**, 925 (2019)
53. N.L.Rosi, J.Eckert, M.Eddaoudi, D.T.Vodak, J.O.Kim, M.O'Keeffe, O.M.Yaghi. *Science*, **300**, 1127 (2003)
54. H.Furukawa, N.Ko, Y.B.Go, N.Aratani, S.B.Choi, E.Choi. *Science*, **329**, 424 (2010)
55. O.K.Farha, I.Eryazici, N.C.Jeong, B.G.Hauser, C.E.Wilmer, A.A.Sarjeant. *J. Am. Chem. Soc.*, **34**, 15016 (2012)
56. M.P.Suh, H.J.Park, T.K.Prasad, D.W.Lim. *Chem. Rev.*, **112**, 782 (2012)
57. M.Felderhoff, C.Weidenthaler, R.von Helmolt, U.Eberle. *Phys. Chem. Chem. Phys.*, **9**, 2643 (2007)
58. H.Reardon, J.M.Hanlon, R.W.Hughes, A.Godula-Jopek, T.K.Mandal, D.H.Gregory. *Energy Environ. Sci.*, **5**, 5951 (2012)
59. S.K.Bhatia, A.L.Myers. *Langmuir*, **22**, 1688 (2006)
60. A.Zuttúl, P.Sudan, P.Mauron, T.Kiyobayashi, C.Emmenegger, L.Schlapbach. *Int. J. Hydrogen Energy*, **27**, 203 (2002)
61. J.Zhou, Q.Wang, Q.Sun, P.Jena, X.S.Chen. *Proc. Natl. Acad. Sci.*, **107**, 2801 (2010)
62. M.A.Obolensky, A.V.Basteev, L.A.Bazyma. *Fullerenes Nanotubes Carbon Nanostructure*, **19**, 133 (2011)
63. M.Yoon, S.Y.Yang, E.Wang, Z.Y.Zhang. *Nano Lett.*, **7**, 2578 (2007)
64. K.Wang, Z.F.Liu, X.Q.Wang, X.D.Cui. *Int. J. Hydrogen Energy*, **39**, 15639 (2014)
65. B.P.Tarasov, M.V.Lototsky, V.A.Yartys. *Russ. J. Gen. Chem.*, **50** (6), 34 (2006)
66. B.Sakintuna, M.Hirscher, F.Lamari. *Int. J. Hydrogen Energy*, **32**, 1121 (2007)
67. B.L.Holmlid. *J. Phys.: Condens. Matter*, **16**, 7017 (2004)
68. J.J.Vajo, S.L.Skeith, F.Mertens. *J. Phys. Chem. B*, **109**, 3719 (2005)
69. A.Zuttel, P.Wenger, S.Rentsch, P.Sudan. *J. Power Sources*, **118**, 1 (2003)
70. G.L.Soloveichik, Y.Gao, J.R.Rijssenbeek, M.Andrus, S.Kniajanski, R.C.J.Bowman, S.J.Hwang, J.C.Zhao. *Int. J. Hydrogen Energy*, **34**, 916 (2009)
71. M.N.Devarakonda, K.P.Brooks, E.Rönnebro, S.D.Rassat. *Int. J. Hydrogen Energy*, **37**, 2779 (2012)
72. H.W.Li, Y.Yan, S.I.Orimo, A.Züttel, C.M.Jensen. *Energies*, **4**, 185 (2011)
73. A.Gutowska, L.Li, Y.Shin, C.M.Wang, X.S.Li, J.C.Linehan. *Angew. Chem., Int. Ed.*, **44**, 3578 (2005)
74. O.V.Komova, N.L.Kayl, G.V.Odegova, O.V.Netskina, V.I.Simagina. *Int. J. Hydrogen Energy*, **41**, 17484 (2016)
75. B.P.Tarasov, M.S.Bocharnikov, Y.A.Yanenko, P.V.Fursikov, M.V.Lototskyy. *Int. J. Hydrogen Energy*, **43**, 4415 (2018)
76. G.Mazzolai. *Int. J. Hydrogen Energy*, **33**, 7116 (2008)
77. N.S.Akhmetov. *Obshchaya i Neorganicheskaya Khimiya*. (General and Inorganic Chemistry). (Moscow: Vysshaya Shkola, 2001)
78. K.E.Lamb, M.D.Dolan, D.F.Kennedy. *Int. J. Hydrogen Energy*, **44**, 3580 (2019)
79. A.Ya. Rozovskii, G.I.Lin. *Teoreticheskie Osnovy Protsessa Sinteza Metenola*. (Theoretical Principles of Methanol Synthesis). (Moscow: Khimiya, 1990)
80. I.Yuranov, N.Autissier, K.Sordakis, A.F.Dalebrook, M.Grasemann, V.Orava, P.Cendula, L.Gubler, G.Layrenczy. *ACS Sust. Chem. Eng.*, **6**, 1 (2018)
81. M.Grasemann, G.Layrenczy. *Energy Env. Sci.*, **5**, 8171 (2012)
82. M.P.Stracke, G.Ebeling, R.Cataluna, J.Dupont. *Energy Fuels*, **21**, 1695 (2007)
83. D.R.MacFarlane, M.Forsyth, P.C.Howlett, M.Kar, S.Passerini, M.Pringle. *Nat. Rev.*, **1**, 1 (2016)
84. N.D.Zelinsky. *Izbrannye Trudy*. (Selected Works). (Moscow, Leningrad: Academy of Sciences of the USSR, 1941)
85. V.N.Ipatieff. *Kataliticheskie Reaktsii pri Vysokikh Temperaturakh i Davleniyakh*: *1900–1933*. (Catalytic Reactions at High Temperatures and Pressures: *1900–1933*). (Moscow, Leningrad: Academy of Sciences of the USSR, 1936)
86. S.M.M.Ehteshami, S.H.Chan. *Energy Policy*, **73**, 103 (2014)
87. Y.Li, J.Song, J.Yang. *Renew. Sust. Energy Rev.*, **42**, 66 (2015)
88. B.K.Koua, P.M.E.Koffi, P.Gbaha, S.Touré. *Renew. Sust. Energy Rev.*, **41**, 907 (2015)
89. L.M.Kustov, A.L.Tarasov, J.Sung, D.Yu.Godovsky. *Mendeleev Commun.*, **24**, 1 (2014)
90. A.Shukla, S.Karmakar, R.B.Biniwale. *Int. J. Hydrogen Energy*, **37**, 3719 (2012)
91. A.Bourane, M.Elanany, T.V.Pham, S.P.Katikaneni. *Int. J. Hydrogen Energy*, **41**, 23075 (2016)
92. U.Rayhan, H.Kwon, T.Yamato. *C.R. Chimie*, **17**, 952 (2014)
93. S.P.Patil, J.V.Pande, R.B.Biniwale. *Int. J. Hydrogen Energy*, **38**, 15233 (2013)
94. D.B.Broom, C.J.Webb, K.E.Hurst, P.A.Parilla, T.Gennett, C.M.Brown. *Appl. Phys. A*, **122**, 151 (2016)
95. Patent US 7101530 (2005)
96. A.V.Talyzin. *Fulleranes*, **2**, 85, (2010)
97. C.B.France, F.A.Frame, B.A.Parkinson. *Langmuir*, **22**, 7507 (2006)
98. R.J.Hamers, S.K.Coulter, M.D.Ellison. *Acc. Chem. Res.*, **33**, 617 (2000)
99. Q.M.Xu, H.Ma, N.Tucker, J.A.Bardecker, K.J.Jen. *Nanotechnology*, **18**, 335302 (2007)
100. F.J.M.Hoeben, P.Jonkheijm, E.W.Meijer, A.P.H.J.Schenning. *Chem. Rev.*, **105**, 1491 (2005)
101. L.Hammett. *Physical Organic Chemistry*. (2nd Edn). (McGraw-Hill, 1970)
102. D.Mackay. In *Physical-Chemical Properties and Environmental Fate for Organic Chemicals*. (Eds D.Mackay, W.Y.Shiu, K.Ch.Ma, S.Ch.Lee). (New York: Taylor and Francis, 2006). P. 925
103. J.D.Roberts, M.C.Caserio. *Basic Principles of Organic Chemistry*. Vol. 1. (2nd Edn). (Menlo Park, CA: W.A.Benjamin, Inc., 1977)
104. S.Nishimura. *Handbook of Heterogeneous Catalytic Hydrogenation for Organic Synthesis*. (New York: Willey, 2001)

105. E.L.Eliel. *Basic Organic Stereochemistry*. (Eds E.L.Eliel, S.H.Wilen, M.P.Doyle). (New York: Willey-Interscience, 2001)
106. A.A.Balandin. *Multipletnaya Teoriya Kataliza. Strukturnye Faktory v Katalize*. (Multiplet Theory of Catalysis. Structural Factors in Catalysis). Pt. 1. (Moscow: Moscow State University, 1963)
107. N.Kariya, A.Fukuoka, T.Utagawa, M.Sakuramoto, Y.Got, M.Ichikawa. *Appl. Catal. A: Gen.*, **247**, 247 (2003)
108. R.B.Biniwale, K.Nobuko, I.Masaru. *Catal. Lett.*, **105**, 83 (2005)
109. M.R.Usman. Ph.D. Thesis. University of Manchester, Manchester, 2008
110. Patent US 3415737 (1968)
111. Gh.Gleichweit. Ph.D. Thesis. Friedrich-Alexander Universität Erlangen, Nürnberg, 2015
112. J.Kehoe, J.Butt. *J. Appl. Chem. Biotechnol.*, **22**, 23 (1972)
113. I.V.Kalechits. *Khimiya Gidrogenizatsionnykh Protsessov v Pererabotke Topliv* (Chemistry of Hydrogenation Processes in Fuel Processing) (Moscow: Khimiya, 1973)
114. R.Van Meerten, T.de Graaf, J.Coenen. *J. Catal.*, **46**, 1 (1977)
115. M.Saeys, M.F.Reyniers, J.W.Thybaut, M.Neurock, G.B.Marin. *J. Catal.*, **236**, 129 (2005)
116. R.K.Herz, W.D.Gillispie, E.E.Petersen, G.A.Somorjai. *J. Catal.*, **67**, 371 (1981)
117. C.T.Campbell, J.M.Campbell, P.J.Dalton, F.C.Henn, J.A.Rodriguez, S.G.Seimanides. *J. Phys. Chem.*, **93**, 806 (1989)
118. Z.V.Zvonkova. *Russ. Chem. Rev.*, **46**, 720 (1977)
119. D.Poondi, M.Vannice. *J. Catal.*, **161**, 742 (1996)
120. M.Temkin, D.Murzin, N.Kulkova. *Kinet. Katal.*, **30**, 637 (1989)
121. J.H.Sinfelt. *J. Mol. Catal. A: Chem.*, **163**, 123 (2000)
122. A.Touzani, D.Klvana, G.Bélanger. *Stud. Surface Sci. Catal.*, **19**, 357 (1984)
123. I.Horiuti, M.Polanyi. *Trans. Faraday Soc.*, **30**, 1164 (1934)
124. P.A.Van Trimpont, G.B.Marin, G.F.Froment. *Appl. Catal. A: Gen.*, **17**, 161 (1985)
125. K.Jouthimurugesan, S.Bhatia, R.D.Srivastava. *Ind. Eng. Chem. Fundam.*, **24**, 433 (1985)
126. M.R.Usman, D.L.Cresswell. *Int. J. Hydrogen Energy*, **10**, 177 (2012)
127. Y.Okada, E.Sasaki, E.Watanabe, S.Hyodo, H.Nishijima. *Int. J. Hydrogen Energy*, **31**, 1348 (2006)
128. R.W.Coughlin, A.Hasan, K.Kawakami. *J. Catal. A*, **88**, 163 (1984)
129. M.J.Sterba, V.Haensel. *Ind. Eng. Chem. Prod. Res. Dev.*, **15**, 2 (1976)
130. M.A.Pacheco, E.E.Petersen. *J. Catal.*, **96**, 507 (1985)
131. H.Belatel, A.H.Kandan, F.A.Khorafi. *Appl. Catal. A: Gen.*, **275**, 141 (2004)
132. N.Boufaden, R.Akkaria, B.Pawelec, J.L.G.Fierro, M.S.Zina, A.Ghorbel. *J. Mol. Catal. A: Chem.*, **420**, 96 (2016)
133. H.P.Steinruck, T.Fuhrmann, C.Papp, B.Trankenschuh, R.Denecke. *J. Chem. Phys.*, **125**, 204706 (2006)
134. C.Gleichweit, M.Amende, O.Höfert, T.Xu, F.Späth, N.Brückner, P.Wasserscheid, J.Libuda, H.P.Steinrück, C.Papp. *J. Phys. Chem. C*, **119**, 20299 (2015).
135. M.Amende, C.Gleichweit, T.Xu, O.Hofert, M.Koch, P.Wasserscheid, H.P.Steinruck, C.Papp, J.Libuda. *Catal. Lett.*, **146**, 851 (2016)
136. H.Jorschik, S.Durr, P.Preuster, P.Wasserscheid. *Energy Technol.*, **7**, 146 (2019)
137. P.Preuster, A.Alekseev, P.Wasserscheid. *Ann. Rev. Chem. Biomol. Eng.*, **8**, 445 (2017)
138. N.Bruckner, K.Obesser, A.Bosmann, D.Teichmann, W.Arlt, J.Dungs. *ChemSusChem.*, **7**, 229 (2014)
139. D.Geburtig, P.Preuster, A.Bosmann, K.Muller, P.Wasserscheid. *Int. J. Hydrogen Energy*, **41**, 1010 (2016)
140. Ch.Krieger, K.Muller, W.Arlt. *Chem. Eng. Technol.*, **39**, 1570 (2016)
141. H.Teichmann, W.Arlt, P.Wasserscheid, R.Freymann. *Int. J. Hydrogen Energy*, **37**, 18118 (2012)
142. F.Sotoodeh, B.J.M.Huber, K.J.Smith. *Int. J. Hydrogen Energy*. **37**, 2715 (2012)
143. F.Sotoodeh, K.J.Smith. *Ind. Eng. Chem.*, **49**, 1018 (2010)
144. L.M.Kustov, A.L.Tarasov, O.P.Tkachenko. *Catal. Lett.*, **148**, 1472 (2018)
145. H.Teichmann, W.Arlt, P.Wasserscheid, R.Freymann. *Energy Environ. Sci.*, **4**, 2767 (2011)
146. M.Amende, C.Gleichweit, K.Werner, S.Schernich, W.Zhao, M.P.A.Lorenz, O.Höfer, C.Papp, M.Koch, P.Wasserscheid, M.Laurin, H.P. Steinrück, J.Libuda. *ACS Catal.*, **4**, 657 (2014)
147. M.Amende, C.Gleichweit, S.Schernich, O.Höfert, M.P.A.Lorenz, W.Zhao, M.Koch, K.Obesser, C.Papp, P.Wasserscheid, H.P.Steinrück, J.Libuda. *J. Phys. Chem. Lett.*, **5**, 1498 (2014)
148. K.M.Eblagon, K.Tam, Yu.Kerry, S.Zhao, X.Q.Gong, H.He. *J. Phys. Chem. C*, **114**, 9720 (2010)
149. M.Yang, C.Han, G.Ni, J.Wu, H.Cheng. *Int. J. Hydrogen Energy*, **37**, 12839 (2012)
150. M.Yang, Y.Dong, S.Fei, H. Ke, H. Cheng. *Int. J. Hydrogen Energy*, **39**, 18976 (2014)
151. A.W.Weitkamp. *Adv. Catal.*, **18**, 1 (1968).
152. P.A.Rautanen. Ph.D. Thesis. Helsinki University of Technology, Espoo, 2002
153. P.A.Rautanen, M.S.Lylykangas, J.R.Aittamaa, A.O.I.Krause. *Stud. Surface Sci. Catal.*, **133**, 309 (2001)
154. P.A.Rautanen, J.R.Aittamaa, A.O.I.Krause. *Chem. Eng. Sci.*, **56**, 1247 (2001)
155. P.Li, Y.L.Huang, D.Chen, J.Zhu, T.J.Zhao, X.G.Zhou. *Catal. Commun.*, **10**, 815 (2009)
156. R.R.Deshmukh, J.W.Lee, U.S.Shin, J.Y.Lee, C.E.Song. *Angew. Chem., Int. Ed.*, **47**, 8615 (2008)
157. A.N.Kalenchuk, D.N.Smetneva, V.I.Bogdan, L.M.Kustov. *Russ. Chem. Bull., Int. Ed.*, **64**, 2642 (2015)
158. B.Wang, D.W.Goodman, G.F.Froment. *J. Catal.*, **253**, 229 (2008)
159. D.Sebastian, C.Alegre, L.Calvillo, M.Perez, R.Moliner, M.Lazaro. *Int. J. Hydrogen Energy*, **39**, 4109 (2014)
160. Y.Okada, K.Imagawa, H.Kawai. *Petrotechnologie*, **38**, 660 (2015)
161. S.L.Gonzalez-Cortes, S.Rugmini, T.Xiao, M.L.H.Green, S.M.Rodulfo-Baechler, F.E.Imbert. *Appl. Catal. A: Gen.*, **475**, 270 (2014)
162. Y.Okada, K.Imagawa, M.Shimura. *Fuel Cell Technol.*, **14**, 36 (2014)
163. S.Hodoshima, S.Takaiwa, A.Shono, K.Satoh, Y.Saito. *Appl. Catal. A: Gen.*, **283**, 235 (2005)
164. L.F.Brown. *Int. J. Hydrogen Energy*, **26**, 381 (2001)
165. D.Sebastian, E.G.Bordeje, L.Calvillo, M.J.Lazaro, R.Moliner. *Int. J. Hydrogen Energy*, **33**, 1329 (2008)
166. G.Lee, Y.Jeong, B.G.Kim, J.S.Han, H.Jeong, H.B.Na, J.C.Jung. *Catal. Commun.*, **67**, 40 (2015)
167. Q.Zhou, P.Li, X.Wang, X.Zhou, D.Yang, D.Chen. *Mater. Chem. Phys.*, **126**, 41 (2011)

168. J.K.S.Nanzhe, R.Rao, M.J.Jin, S.E.Park. *Appl. Catal. A: Gen.*, **425** – **426**, 62 (2012)
169. C.M.Lu, Y.M.Lin, I.Wang. *Appl. Catal. A: Gen.*, **198**, 223 (2000)
170. E.Sahle-Demessie, V.G.Devulapelli, A.A.Hassan. *Catalysts*, **2**, 85 (2012)
171. R.Abu-Reziq, D.Avnir, I.Miloslavski, H.Schumann, J.Blum. *J. Mol. Catal. A: Chem.*, **185**, 179 (2002)
172. I.S.Park, M.S.Kwon, K.Y.Kang, J.S.Lee, J.Park. *Adv. Synth. Catal.*, **349**, 2039 (2007)
173. E.Bresó-Femenia, B.Chaudret, S. Castillón. *Catal. Sci. Technol.*, **5**, 2741 (2015)
174. Z.G.Zhang, T.Yoshida. *Energy Fuels*, **15**, 708 (2001)
175. L.B.Sun, X.Y.Wei, X.Q.Liu, Z.M.Zong, W.Li, J.H.Kou. *Energy Fuels*, **23**, 4877 (2009)
176. J.L.Pinilla, A.B.Garcia, K.Philippot, P.Lara, E.J.Garcia-Suarez, M.Millan. *Fuel*, **116**, 729 (2014)
177. V.Kogan, Z.Aizenshtata, R.Neumann. *New J. Chem.*, **26**, 272 (2002)
178. A.N.Kalenchuk, A.E.Koklin, V.I.Bogdan, L.M.Kustov. *Russ. Chem. Bull., Int. Ed.*, **67**, 1406 (2018)
179. A.N.Kalenchuk, A.E.Koklin, V.I.Bogdan, V.V.Lunin. *Russ. J. Phys. Chem. A*, **92**, 663 (2018)
180. P.Castano, D.van Herk, M.T.Kreutzer, J.A.Moulijn, M.Makkee. *Appl. Catal. B: Env.*, **88**, 213 (2009)
181. A.N.Kalenchuk, A.E.Koklin, V.I.Bogdan, L.M.Kustov. *Russ. Chem. Bull., Int. Ed.*, **66**, 1208 (2017)
182. W.Brugel, E.Kuss, T.Pollmann, H.Stegemeyer. *J. Mol. Struct.*, **1**, 61 (1967)
183. A.N.Kalenchuk, V.I.Bogdan, S.F.Dunaev, L.M.Kustov. *Fuel Proc. Technol.*, **169**, 94 (2018)
184. M.A.V.Ribeiro da Silva, L.M.N.B.F.Santos, S.Spencer, L.M.Lima. *J. Chem. Thermodyn.*, **40**, 375 (2008)
185. A.N.Kalenchuk, V.I.Bogdan, S.E.Bogorodskii, L.M.Kustov. *Kinet. Catal.*, **57**, 219 (2016)
186. A.N.Kalenchuk, V.I.Bogdan, S.F.Dunaev, L.M.Kustov. *Chem. Eng. Technol.*, **41**, 1842 (2018)
187. L.M.Kustov, A.N.Kalenchuk, S.F.Dunaev, V.I.Bogdan. *Mendeleev Commun.*, **29**, 25 (2019)
188. A.N.Kalenchuk, N.A.Davshan, V.I.Bogdan, S.F.Dunaev, L.M.Kustov. *Russ. Chem. Bull., Int. Ed.*, **67**, 28 (2018)